WMO Typhoon Committee
Roving Seminar 2023

Role of midlatitude baroclinic condition in heavy rainfall events directly induced by tropical cyclones in South Korea

Chanil Park

Post-doctoral scholar
School of Earth and Environmental Sciences
Seoul National University

Collaboration with:
Prof. Seok-Woo Son (SNU)
Dr. Eun Jeong Cha (NIMS)
Prof. Yukari Takayabu (U. Tokyo)
Prof. Sang-Hun Park (Yonsei U.)
Prof. Dong-Hyun Cha (UNIST)

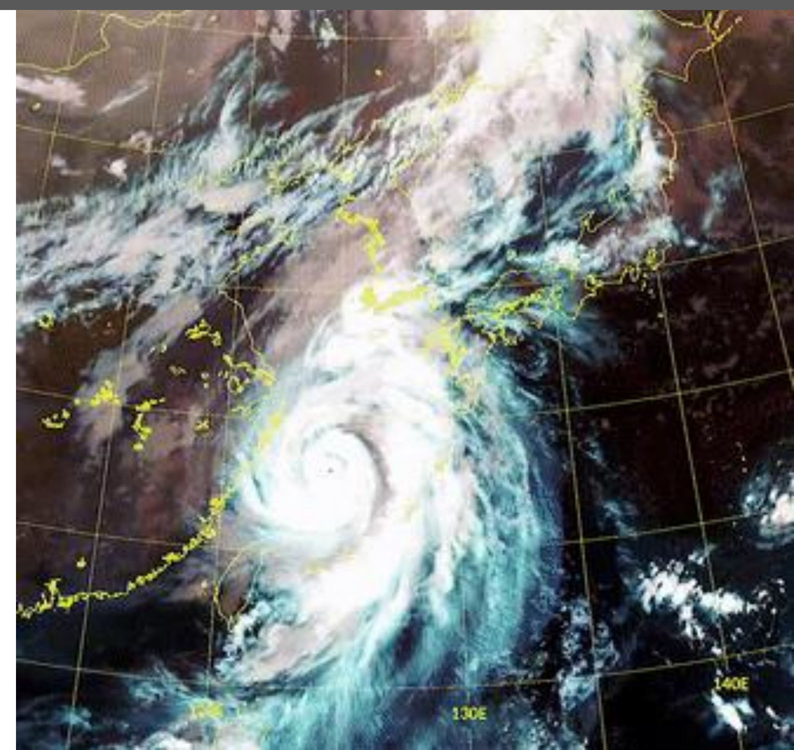

This work was funded by the Korea Meteorological Administration Research and Development Program "Advancing Severe Weather Analysis and Forecast Technology" under Grant (KMA2018-00121).

Tropical cyclone vs. Extratropical cyclone

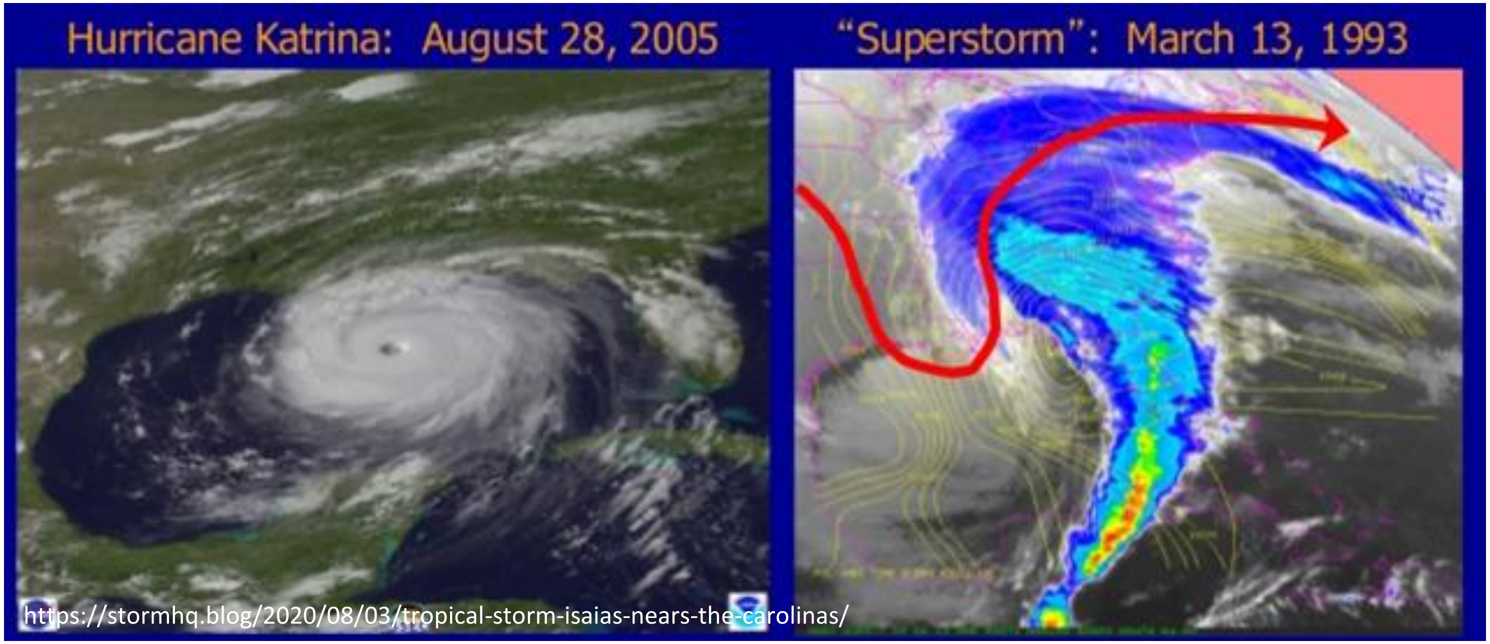

	Tropical cyclone	Extratropical cyclone
Energy sources	Latent heat release from warm SST through deep moist convection	Large temperature gradient (mean APE) and their zonal asymmetry (eddy APE)
Vertical structure	Upright (barotropic), warm core	Westward tilt (baroclinic), cold core
Wind / precipitation / temperature fields	Almost axisymmetric, non-frontal	Asymmetric, frontal

Extratropical transition (ET)

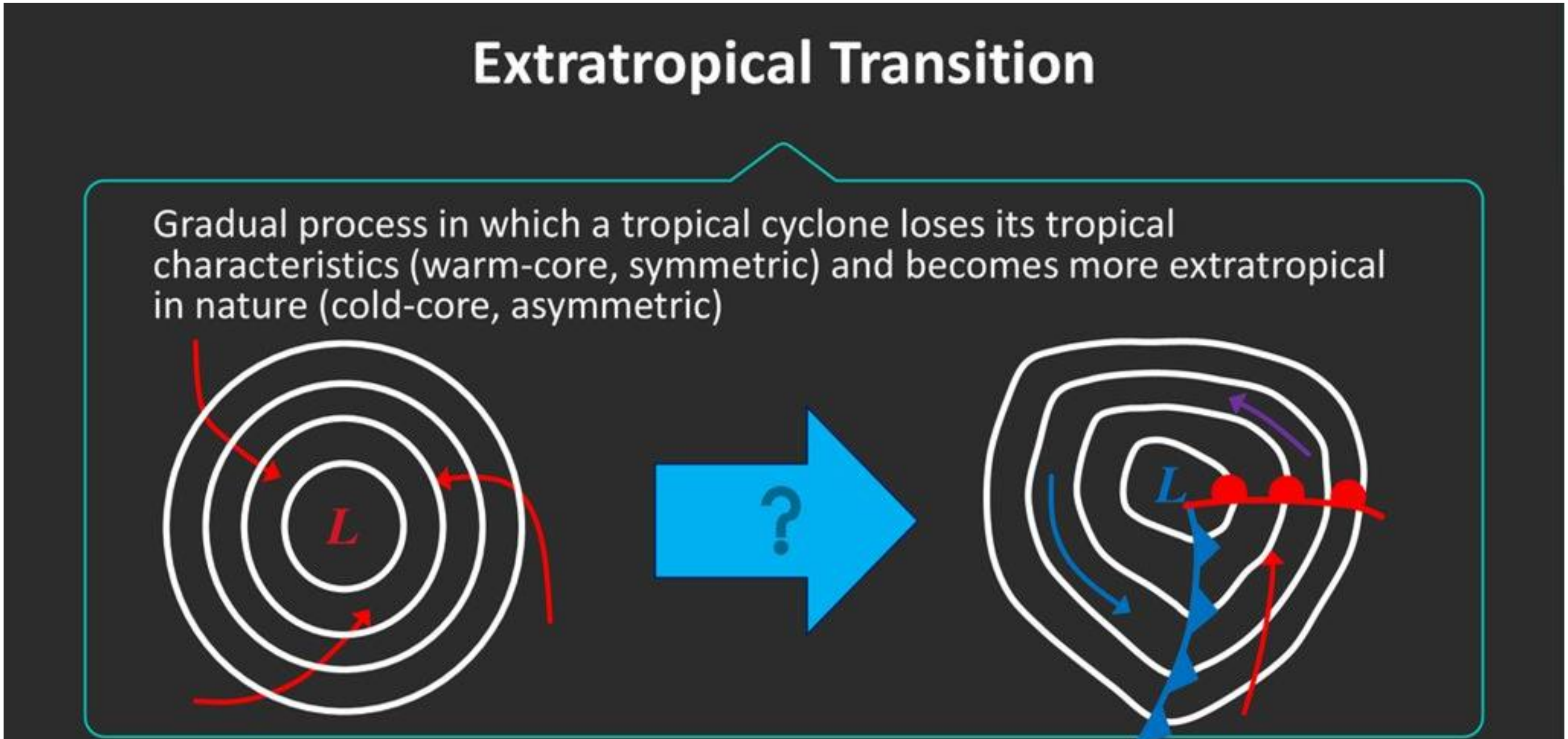

https://slideplayer.com/slide/15855244/

Climatology of ET

Track of TCs completing ET in four ocean basins

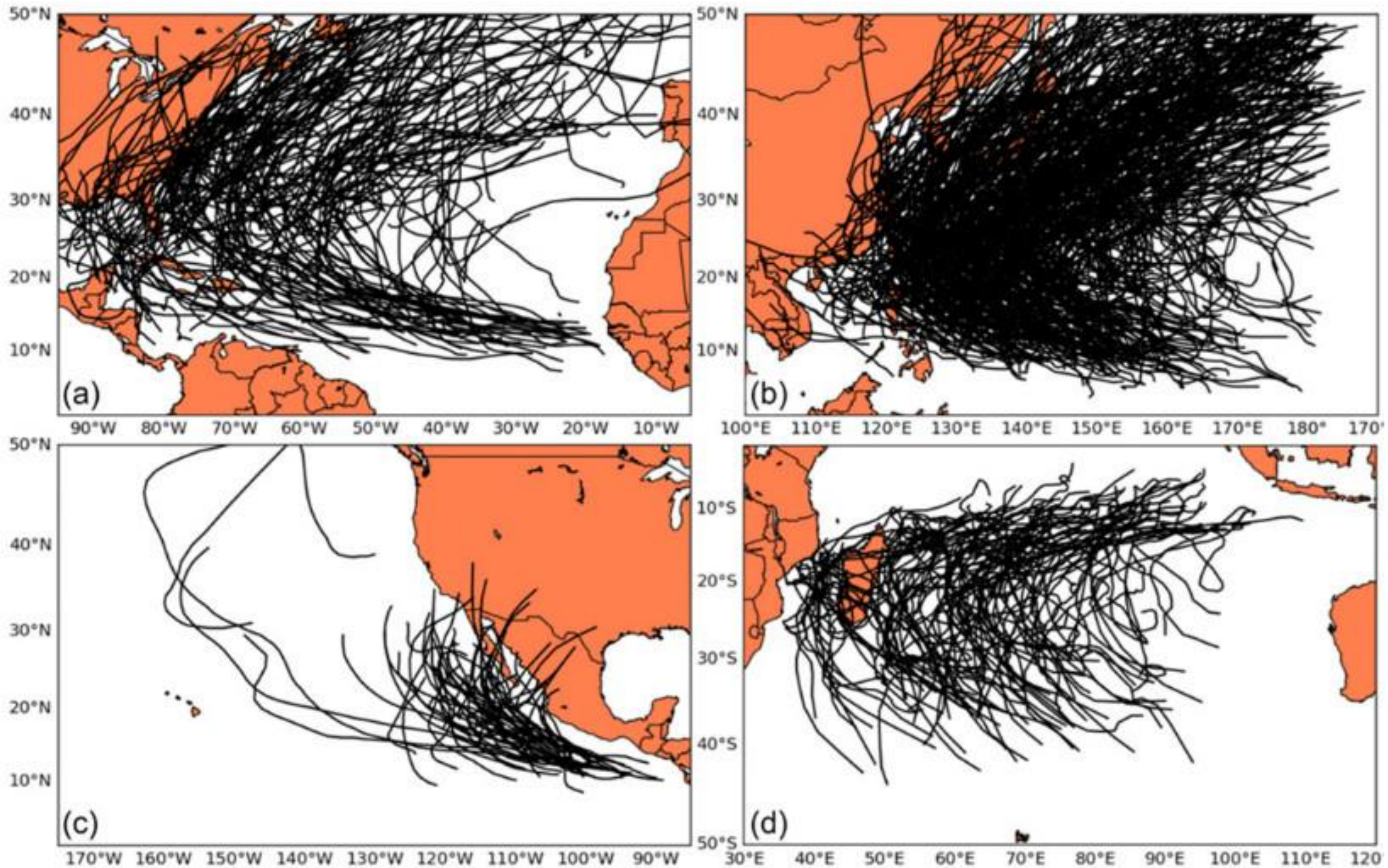

Keller et al. (2019)

- ET occurs in all TC-generating ocean basins.
- ET is relatively rare in the eastern North Pacific (cold California Current & North American monsoon) but most frequent in the western North Pacific.

Climatology of ET

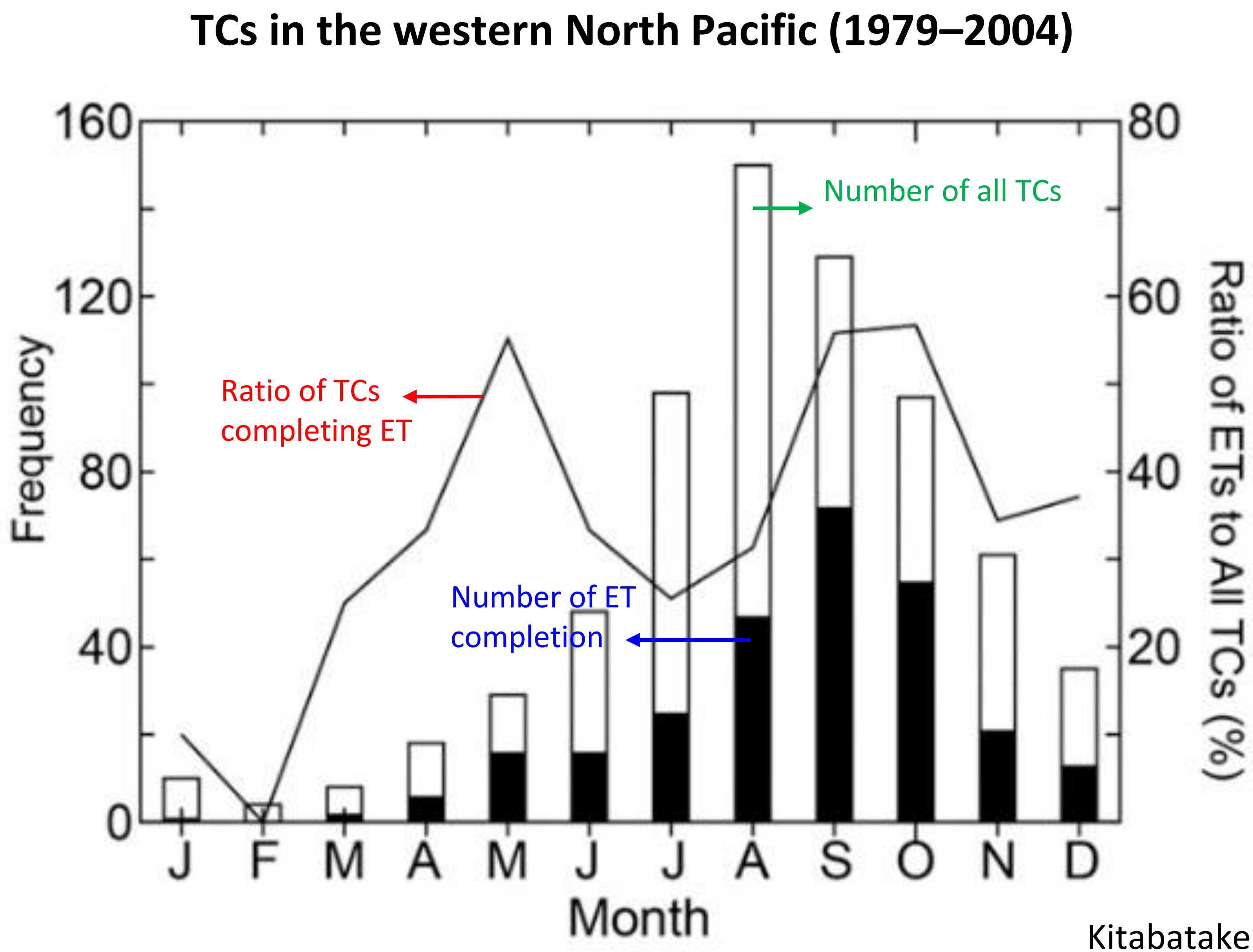

Kitabatake (2011)

Climatology of ET

TCs in the western North Pacific (1979–2020)

TCs approaching East Asia
(ET completion: 85.9%)

TCs approaching Southeast Asia
(ET completion: 7.4%)

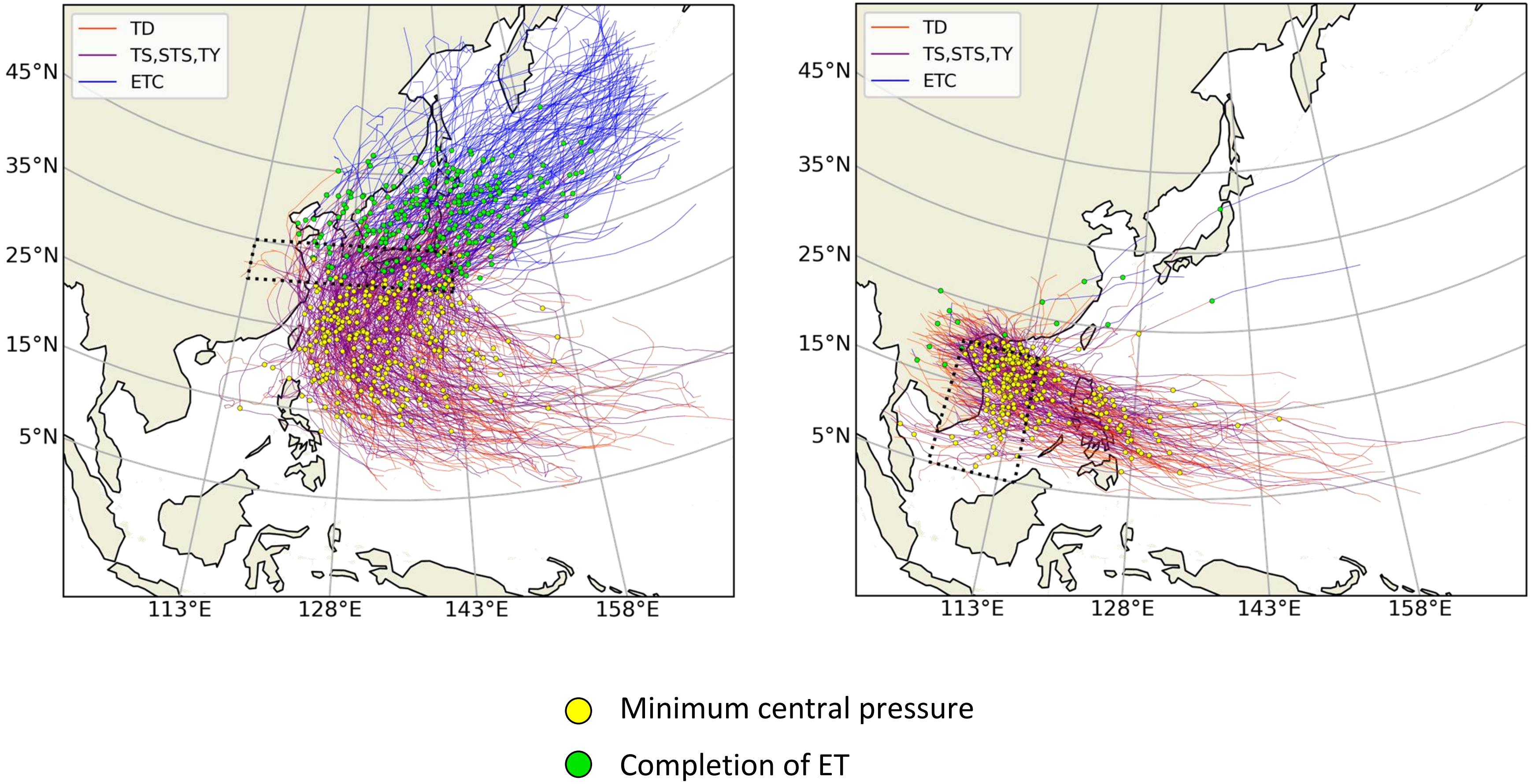

Literature review of ET

Two asepcts of ET dynamics

1. Structural changes of TCs

Klein et al. (2000)

2. Modification of midlatitude flows

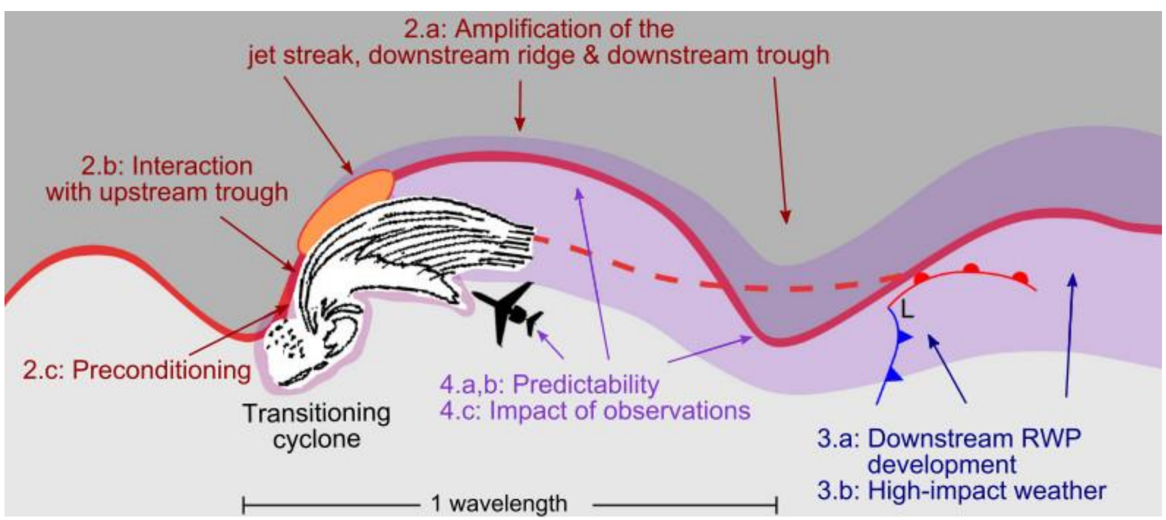

Keller et al. (2019)

Structural changes of TCs: Transformation stage

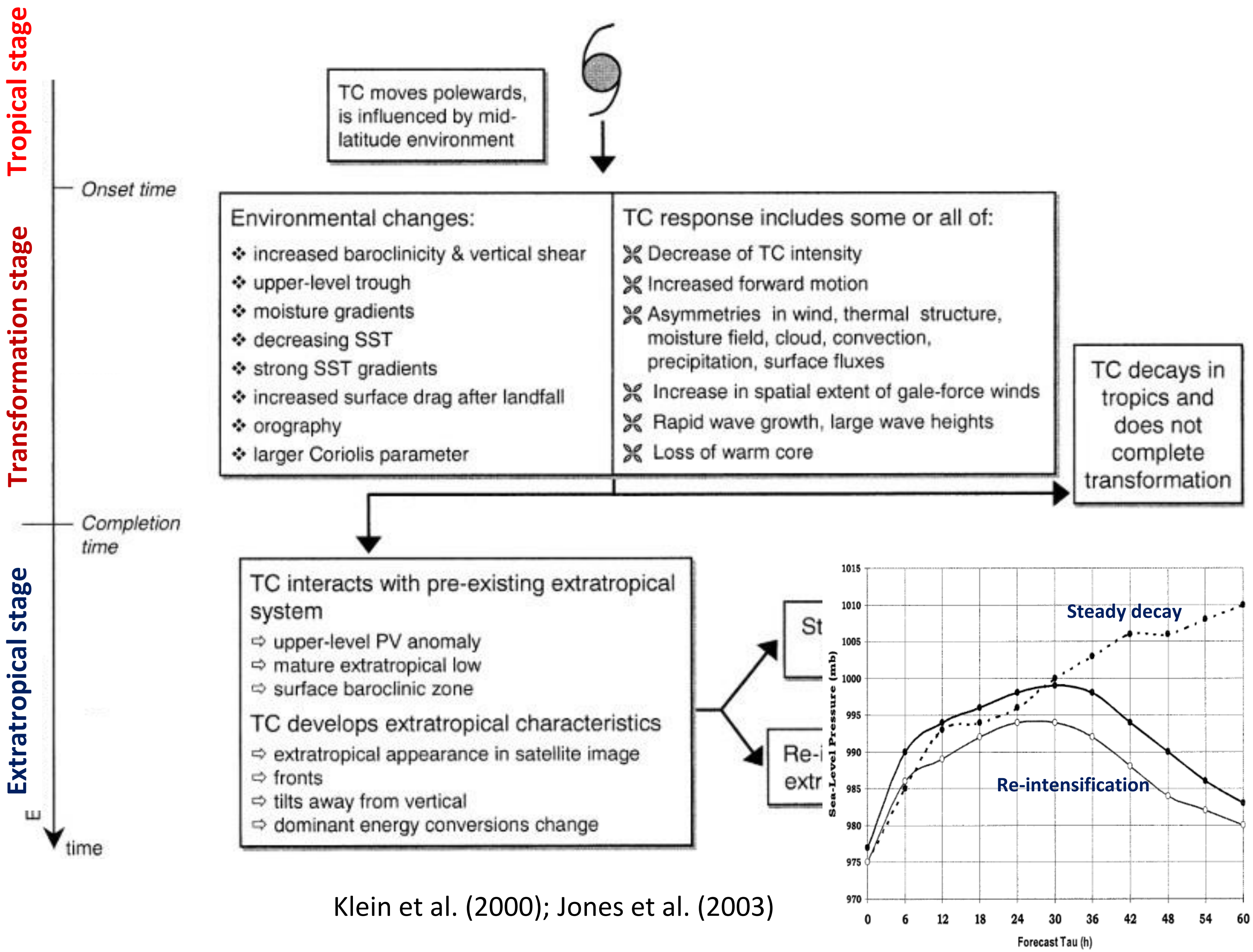

Klein et al. (2000); Jones et al. (2003)

Structural changes of TCs: Transformation stage

Transformation stage of ET
(now, simply ET)

- **Step 1:** Expansion of precipitating field outward of TC inner core. Development of asymmetric cloud structure along with dry-air intrusion from high-latitude upper troposphere.

- **Step 2:** Interaction between upper-level outflow and pre-existing midlatitude jet stream. Development of large-scale cloud shield to the north/northeast of TC.

- **Step 3:** Erosion of eyewall convection and warm-core structure. Development of warm-frontal structure to the northeast.

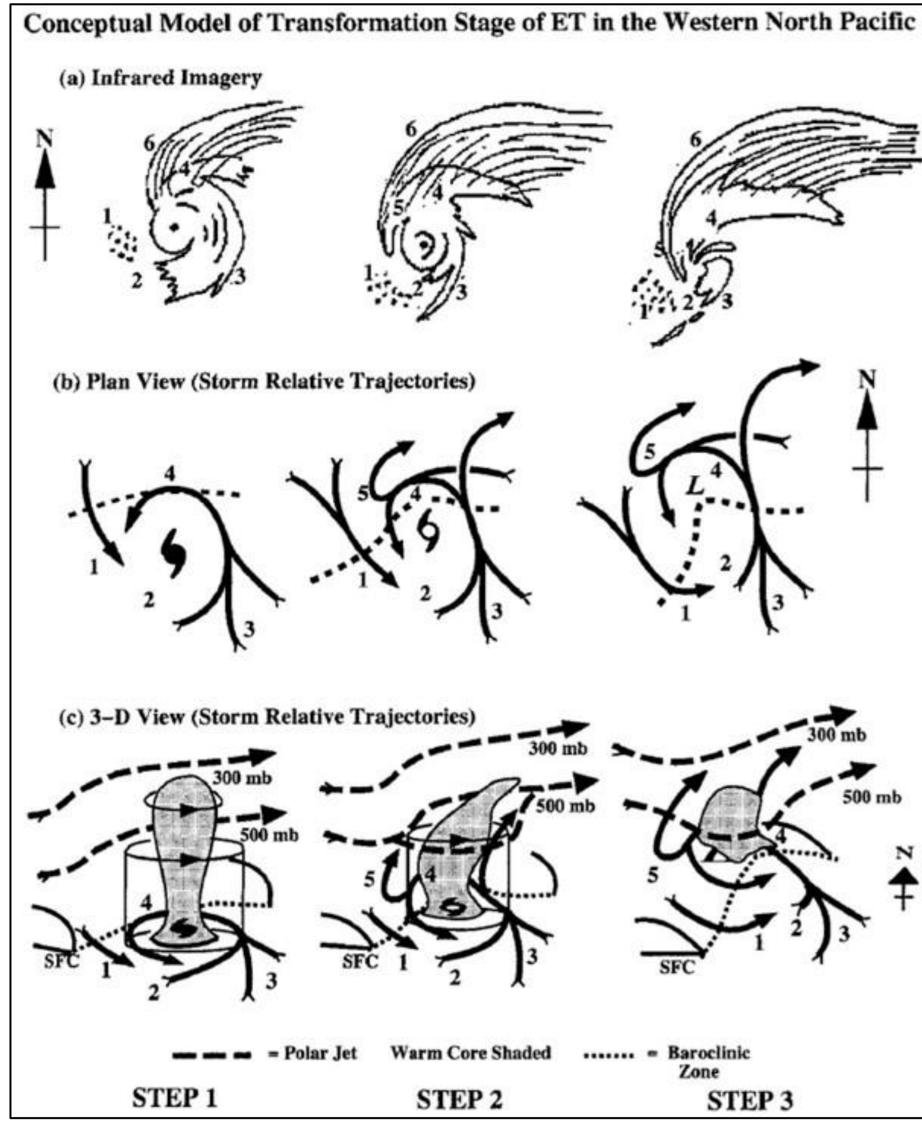

Klein et al. (2000)

Structural changes of TCs: Satellite images

Ginger (1997)

Stella (1998)

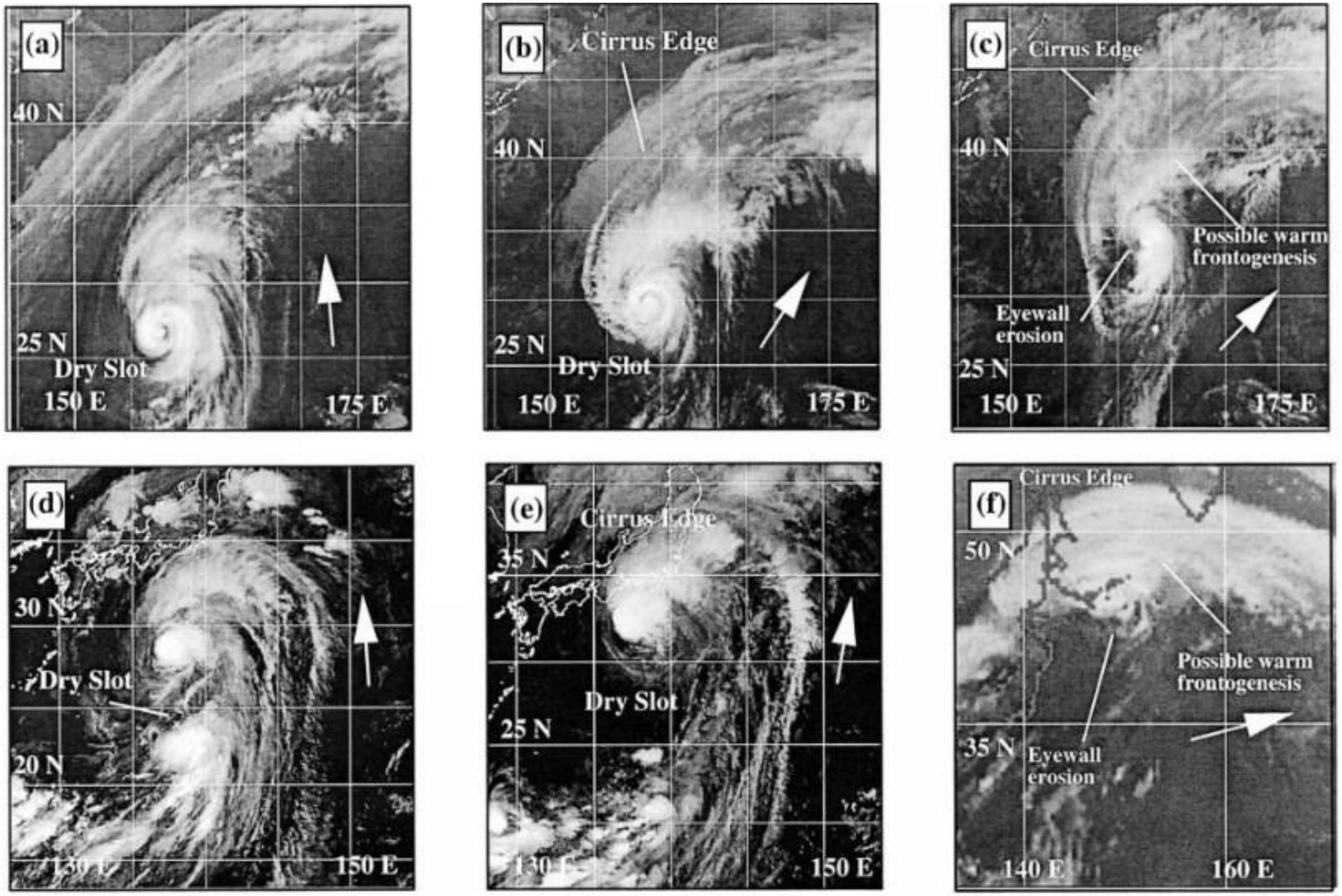

Klein et al. (2000)

Structural changes of TCs: Satellite images

Hinnamnor (2022)

0600 KST 4 Sep

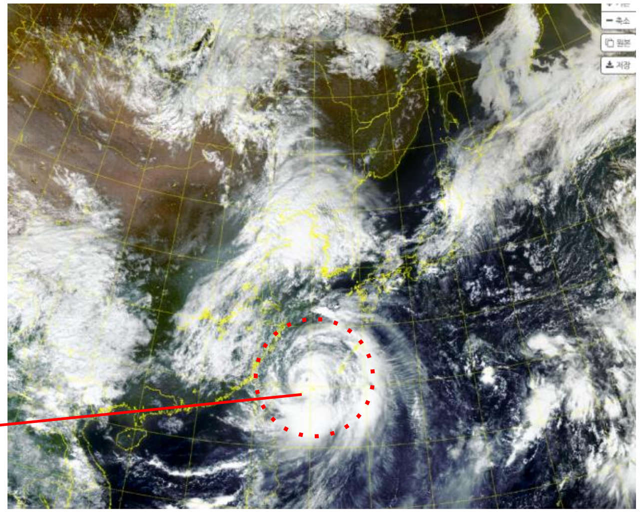

Spiral cloud band

0600 KST 5 Sep

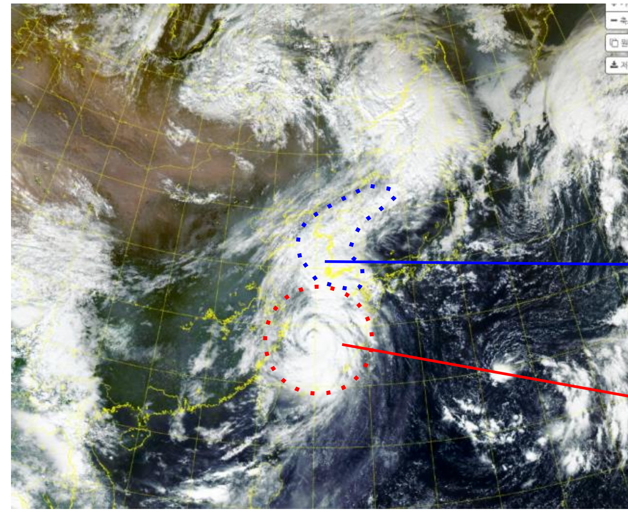

TC-ahead Rain shield

Spiral cloud band

0600 KST 6 Sep

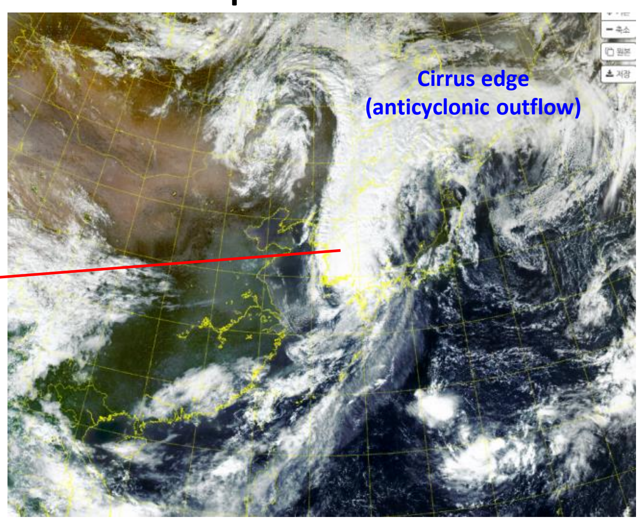

Erosion of eyewall convection, spiral cloud band

0600 KST 7 Sep

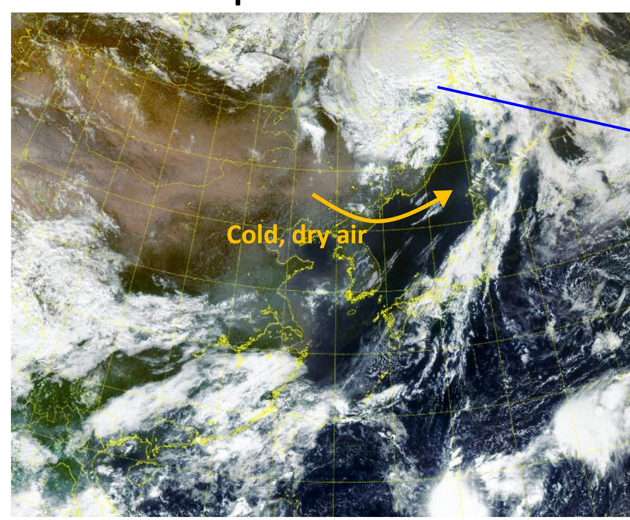

Extratropical cyclone (completion of ET)

KMA National Meteorological Satellite Center

Structural changes of TCs: Upward motion

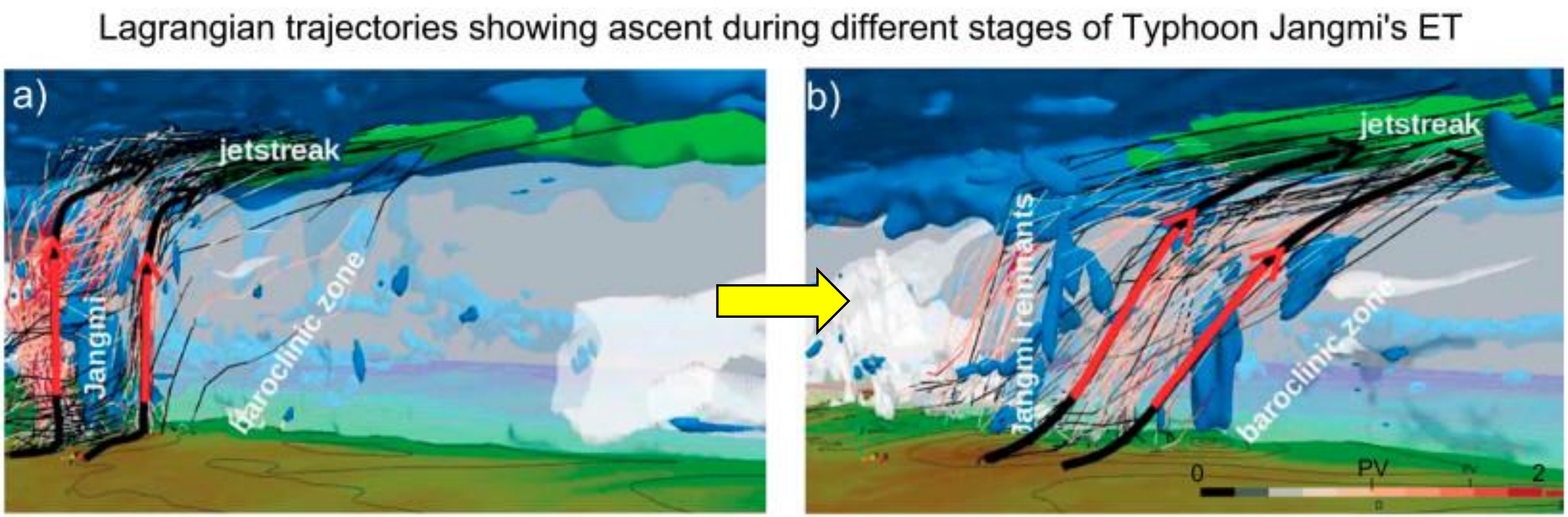

Grams et al. (2013)

- In the early stage of ET, the upright TC convection is replaced by the slantwise ascent, whose center deviates poleward from the TC center.
- This indicates the development of *warm conveyor belt along the moist isentropes* in midlatitudes.

Structural changes of TCs: Wind fields

Wind speed, frontal uplift at 700 hPa

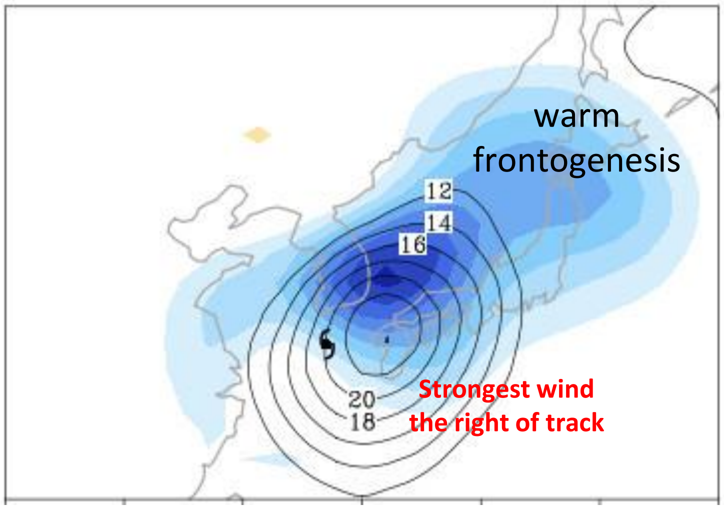

Park et al. (2023, in revision)

Azimuthally averaged tangential wind

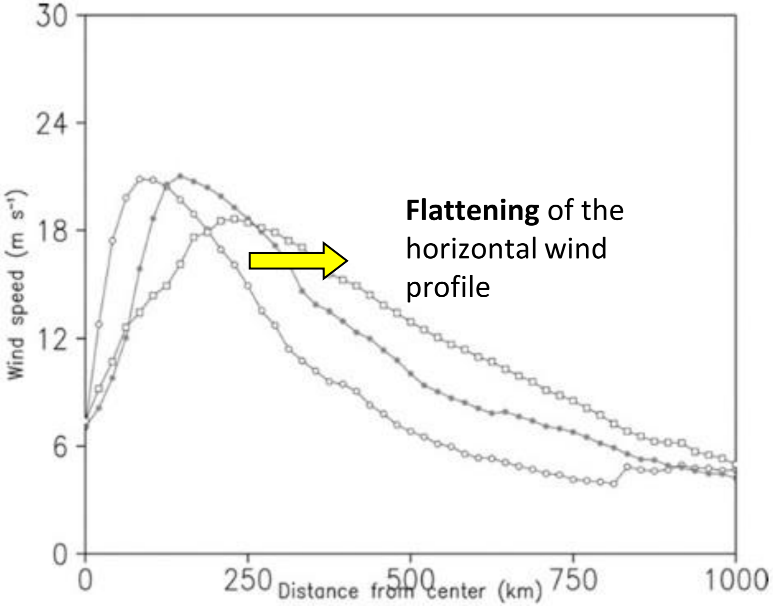

Evans and Hart (2008)

- Near-surface wind field becomes *increasingly asymmetric* (Powell 1982; Merrill 1993).
- The strongest winds appears to the right of track, developing the *warm frontal zone* to the north/northeast.

- The maximum wind speed decreases, but the radius of maximum wind speed increases (size expansion of storms' impact range).

Structural changes of TCs: Phasing with upstream trough

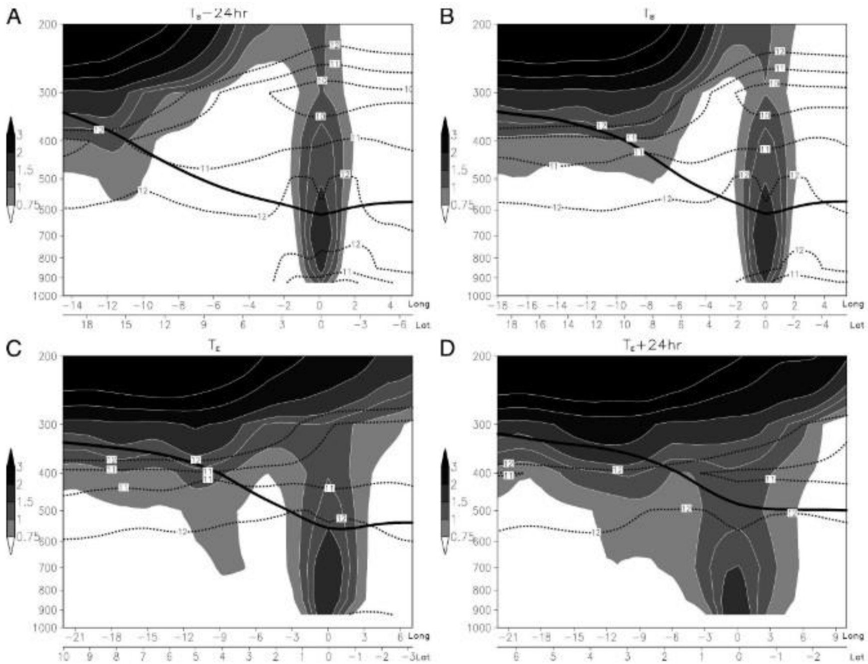

Hart et al. (2006)   Shading: PV, contours: isentrope

$$\left(\sigma_0 \nabla^2 + f_0^2 \frac{\partial^2}{\partial p^2}\right) \omega \approx 2 f_0 \frac{\partial \mathbf{v}_g}{\partial p} \cdot \nabla \zeta_g$$

- ET and post-ET re-intensification is catalyzed if TCs are properly phased with upstream upper-level tough in midlatitudes.
- Petterssen–Smebye Type-B cyclogenesis (Petterssen and Smebye 1971).

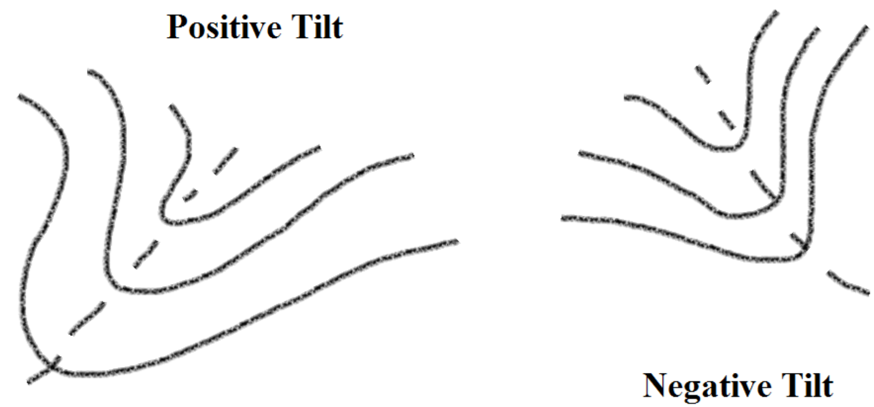

- Negatively-tilted trough is more favorable for post-ET re-intensification (Hart et al. 2006; Milrad et al. 2009).
- Proper phasing is more important than the intensity of trough (Ritchie and Elsberry 2003; Ritchie et al. 2007).

Structural changes of TCs: Cyclone phase space

Cyclone phase space (CPS) (Hart 2003)

Hart (2003) proposed a CPS diagram to quantify and visualize the structural changes of TCs, and thereby to objectively determine the onset/completion of ET.

- **Thermal symmetry** (B)

$$B = h\left[\overline{(Z_{600\,hPa} - Z_{900\,hPa})}\big|_R - \overline{(Z_{600\,hPa} - Z_{900\,hPa})}\big|_L\right]$$

10 m

Symmetric ⟷ Asymmetric

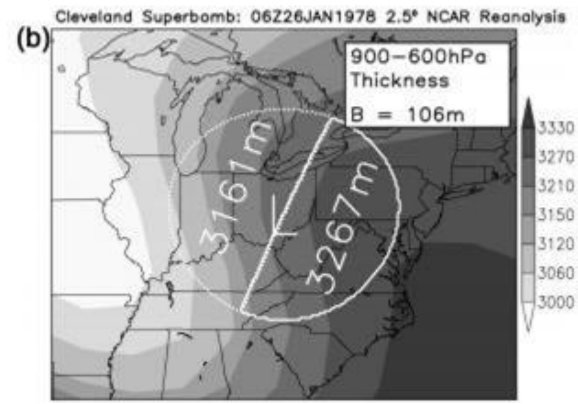

- **Upper and low-level thermal winds** $(-V_T^U, -V_T^L)$

$$-V_T^L = \frac{\partial \Delta Z}{\partial \ln p}\bigg|_{900\,hPa}^{600\,hPa}, \quad -V_T^U = \frac{\partial \Delta Z}{\partial \ln p}\bigg|_{600\,hPa}^{300\,hPa}$$

where $\Delta Z = Z_{max} - Z_{min}$

0

Cold core ⟷ Warm core

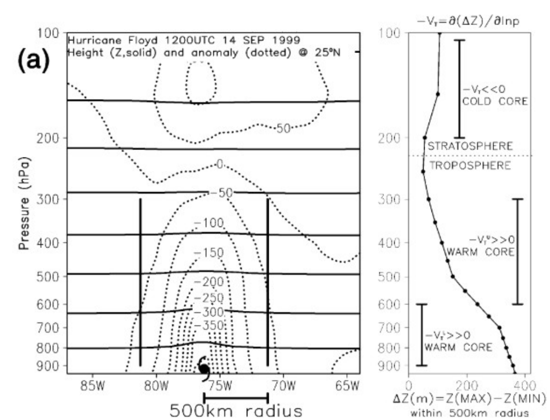

Structural changes of TCs: Cyclone phase space

Cyclone phase space (CPS) (Hart 2003)

Example: Hinnamnor (2022)

$-V_T^L$ vs B

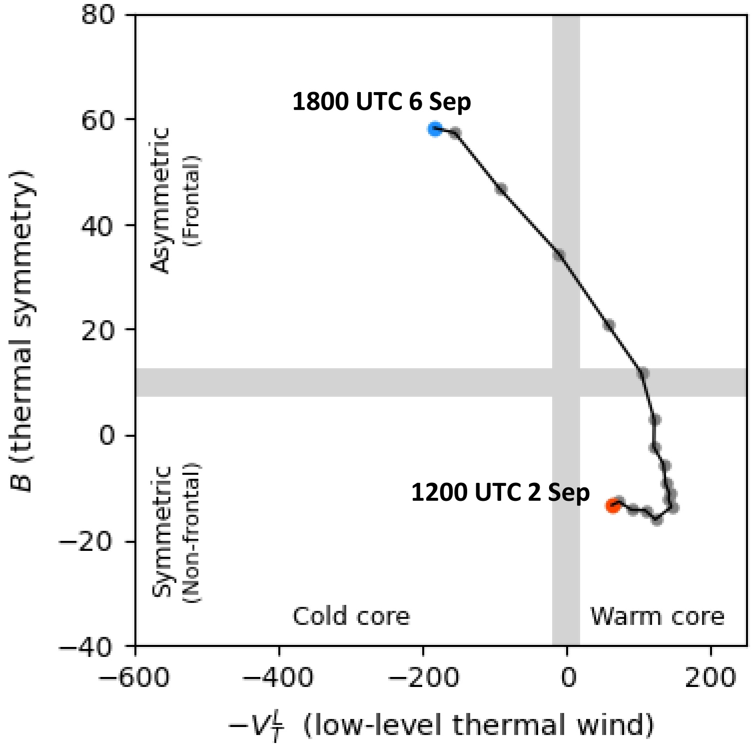

$-V_T^L$ vs $-V_T^U$

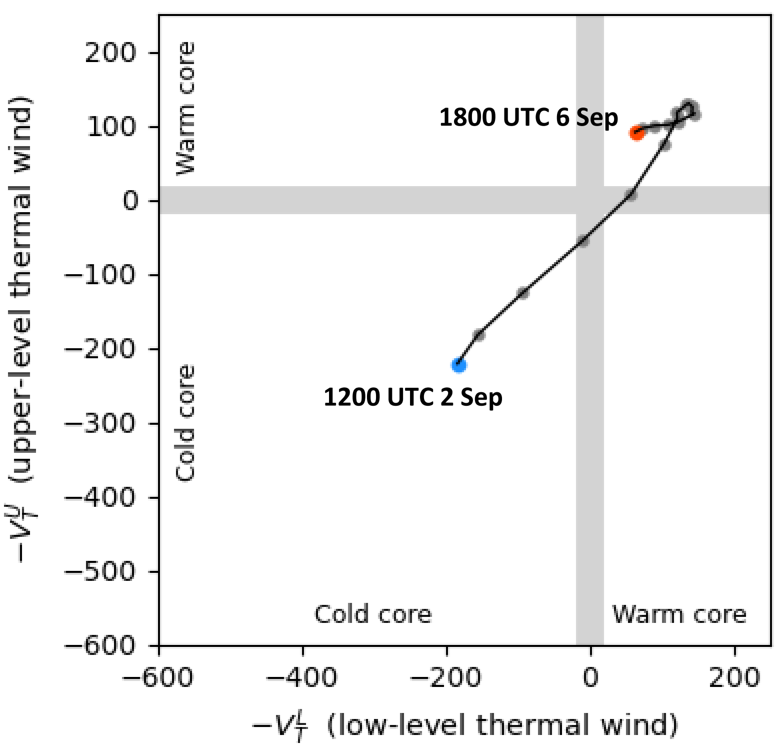

Two asepcts of ET dynamics

1. Structural changes of TCs

Klein et al. (2000)

2. Modification of midlatitude flows

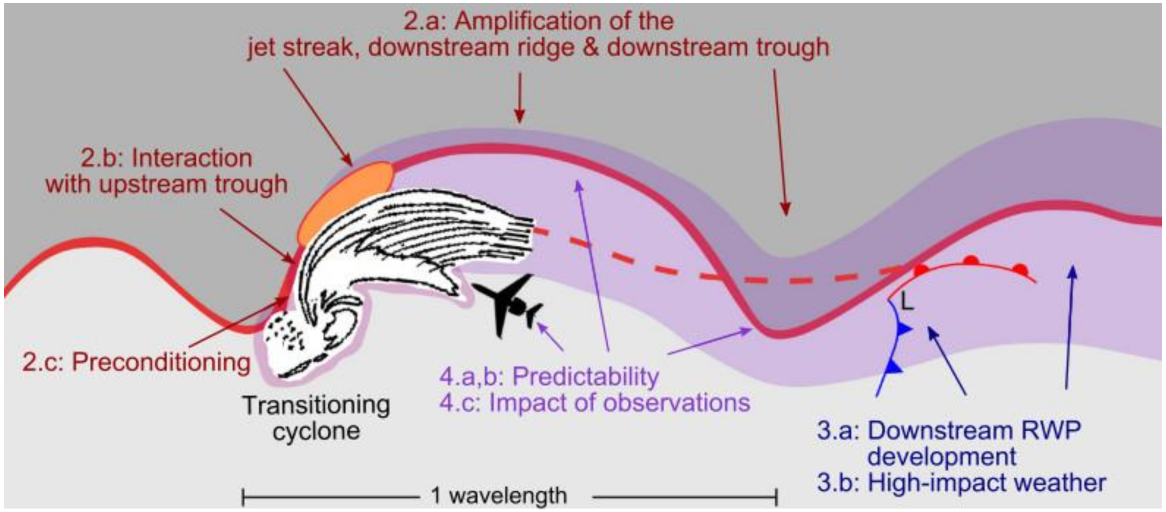

Keller et al. (2019)

Modification of midlatitude flows: Vicinity of TCs

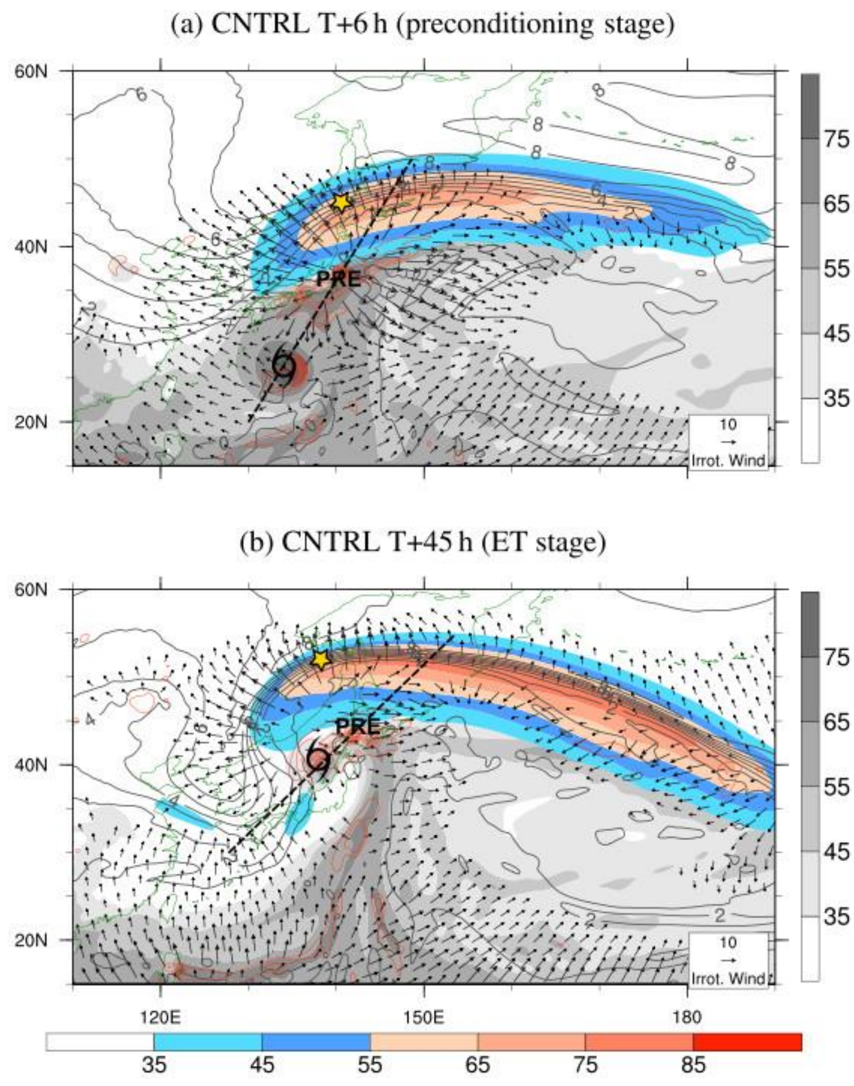

Grams and Archambault (2016)

- As TCs approach baroclinic zones, downstream ridge builds and jet amplifies in the upper troposphere.

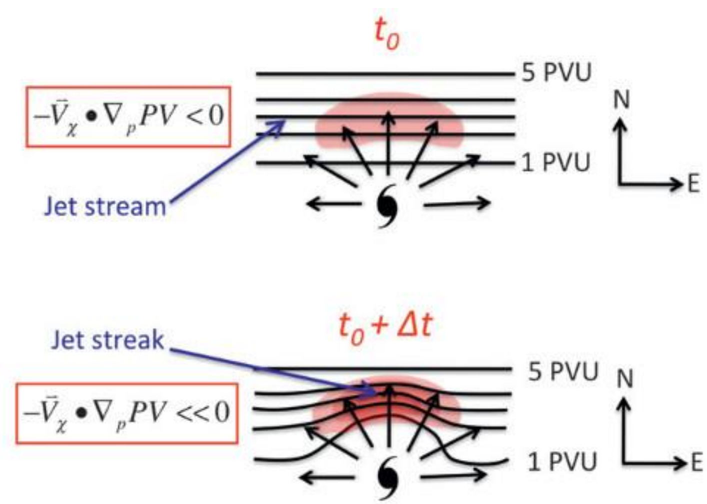

Archambault et al. (2013)

- A key process is divergent TC outflow in the upper troposphere.
- An upstream midlatitude trough is often decelerated by the TC out flow, leading to the TC-trough juxtaposition.

Modification of midlatitude flows: Downstream development

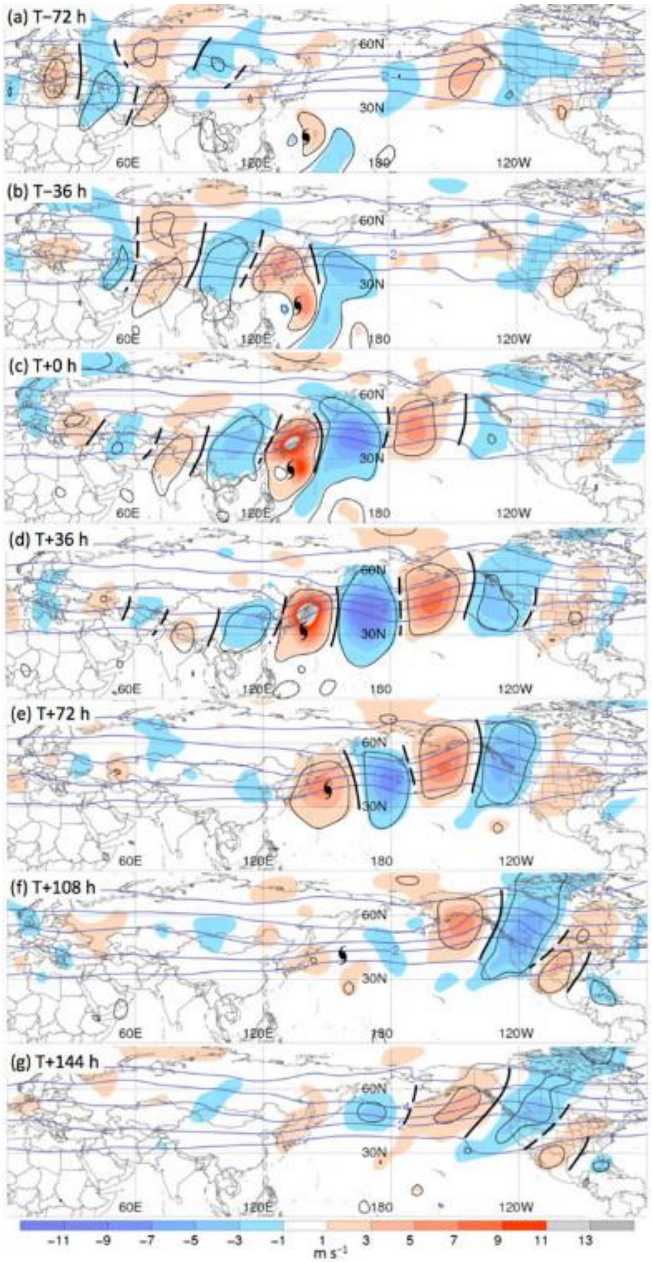

- TCs' influence on midlatitude flows is not confined to their vicinity, but extend far downstream through baroclinic Rossby wave dispersion.

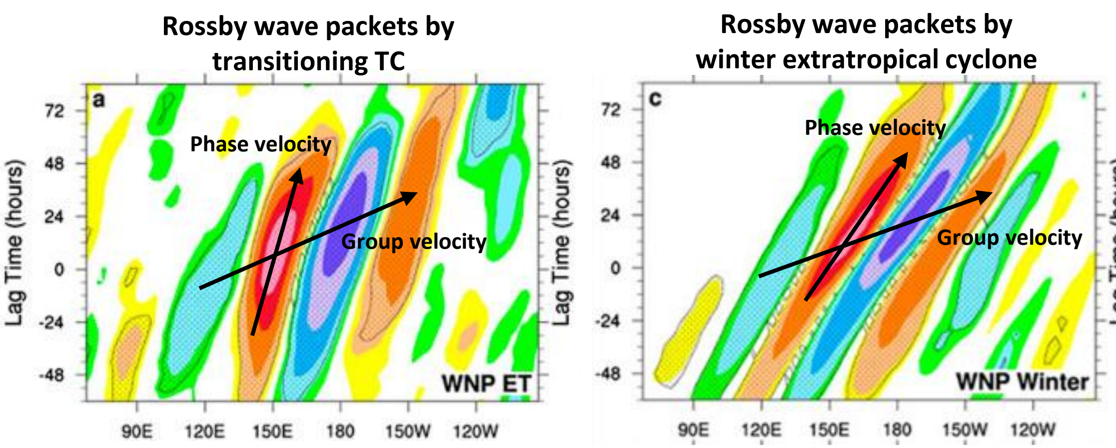

Torn and Hakim (2015)

- Rossby waves emanated from transitioning TC has smaller c_p (phase velocity) compared to those related to midlatitude storm track.

Archambault et al. (2015)

Modification of midlatitude flows: Interaction strength

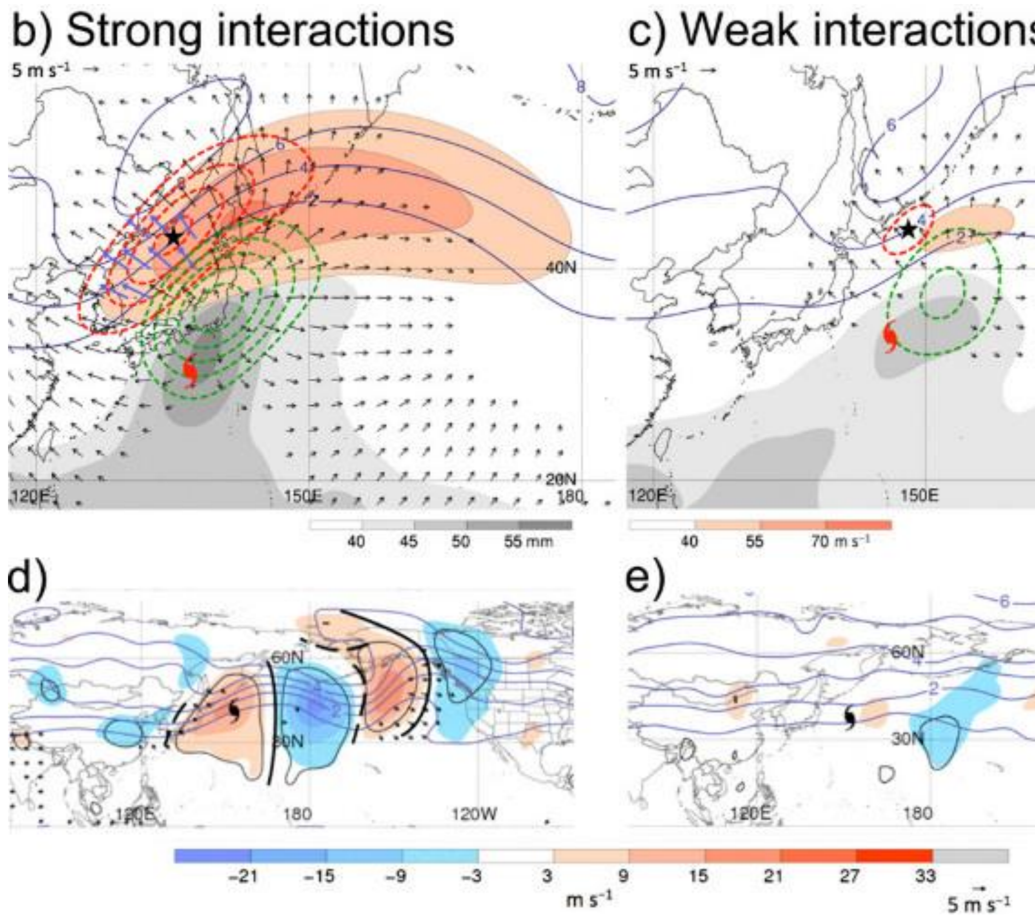

Archambault et al. (2015)

- Stronger TC–midlatitude flow interaction in the vicinity of TC assures the more amplified downstream development.

Modification of midlatitude flows: Weather impacts

Nuri (2014)

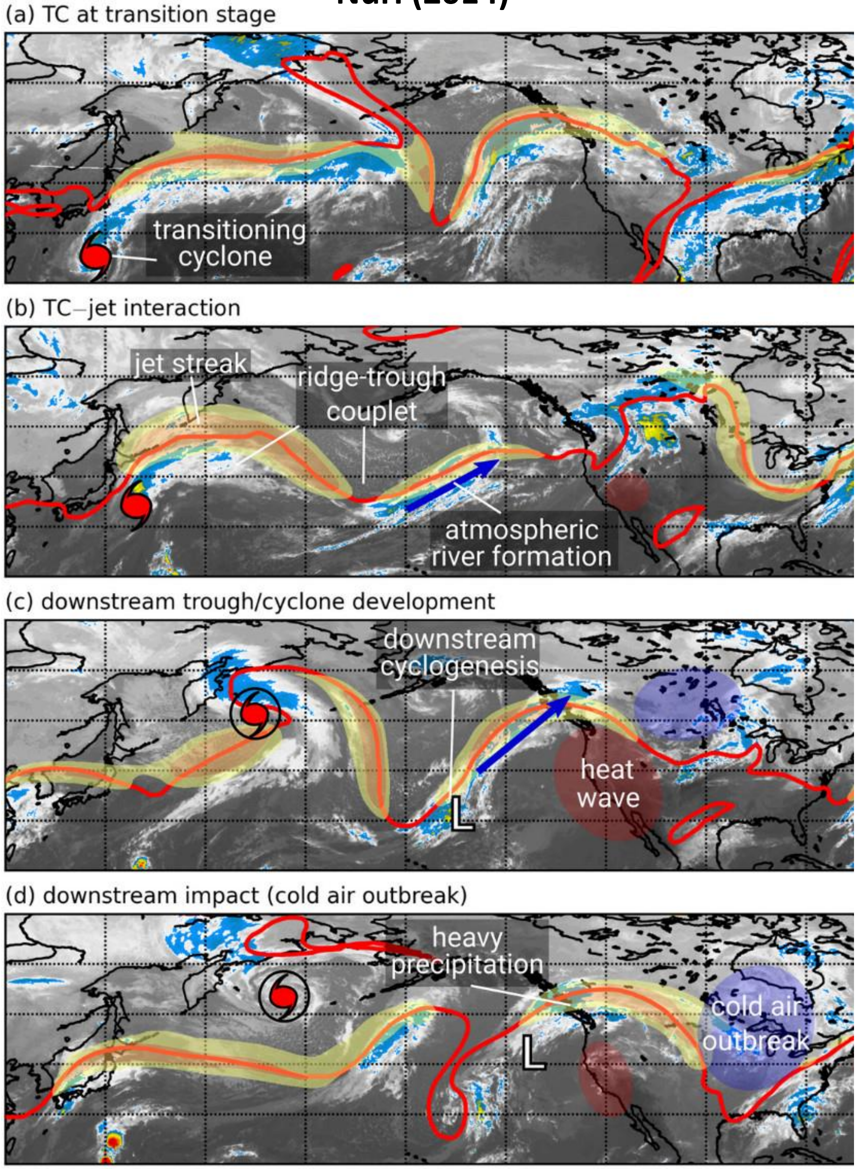

Keller et al. (2019)

- ET-induced downstream development sometimes causes secondary severe weather events.
  - ✓ Downstream cyclogenesis
  - ✓ Atmospheric river formation
  - ✓ Heat wave
  - ✓ Blocking high
  - ✓ Cold air outbreak

Modification of midlatitude flows: Source of forecast errors

Nuri (2014)

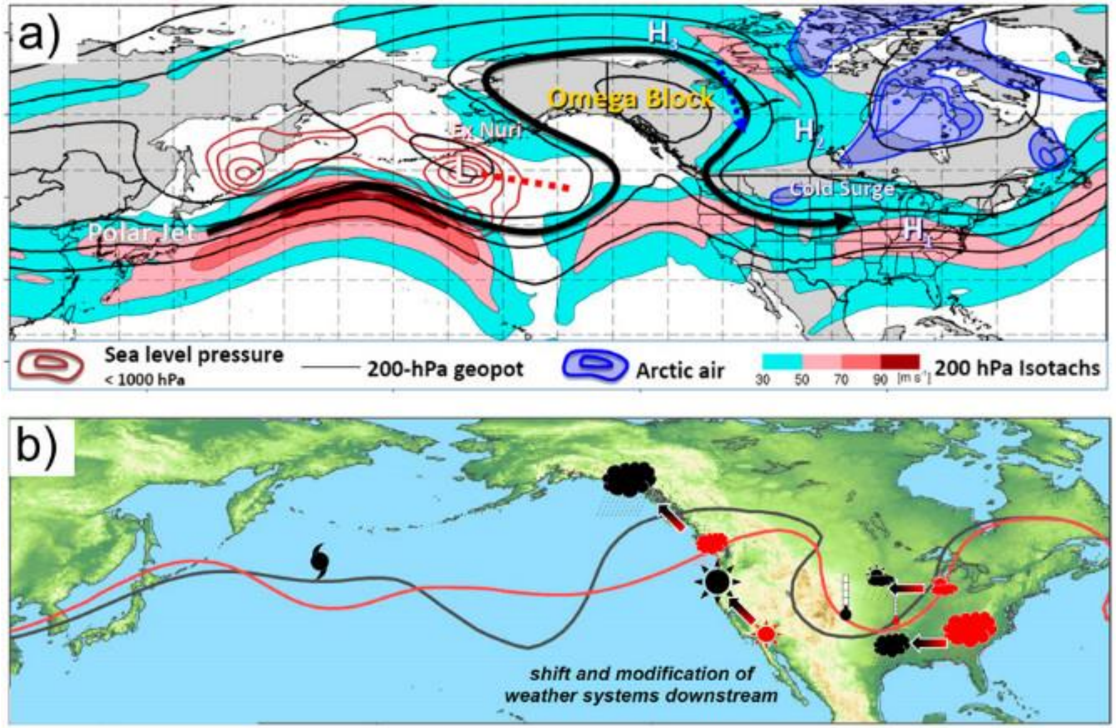

Keller et al. (2019)

Inter-ensemble standard deviation of Z500 (Hurricane Ike 2008)

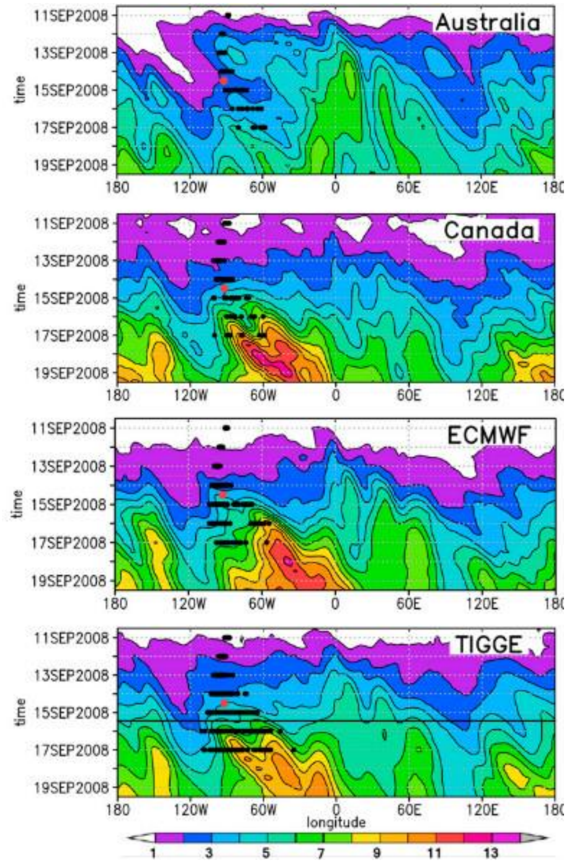

Keller et al. (2011)

- Incorrect representation of the 1) phasing between the transitioning TCs and the upstream trough and 2) diabatic processes lead to large errors in downstream weather forecasts.

Modification of midlatitude flows: Mechanisms

- **Potential vorticity (PV) framework** (Archambault et al. 2013, 2015; Grams and Archambault 2016; Riboldi et al. 2019)

$$\frac{\partial P}{\partial t} = -\mathbf{V}_{\chi}\cdot\nabla P - \mathbf{V}_{\psi}\cdot\nabla P - \omega\frac{\partial P}{\partial p} - g\left[(\zeta+f)\frac{\partial\dot{\theta}_{Dia}}{\partial p} + \frac{\partial\dot{\theta}_{Dia}}{\partial y}\frac{\partial u}{\partial p} - \frac{\partial\dot{\theta}_{Dia}}{\partial x}\frac{\partial v}{\partial p}\right]$$

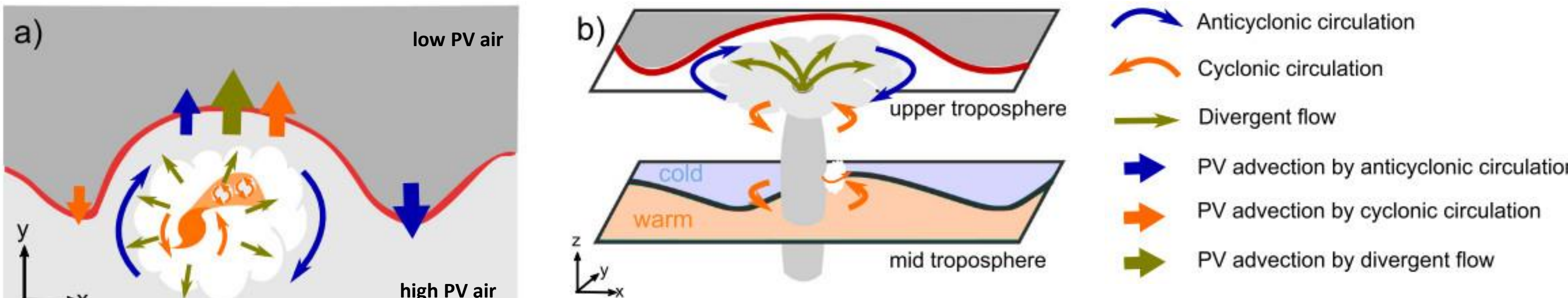

Keller et al. (2019)

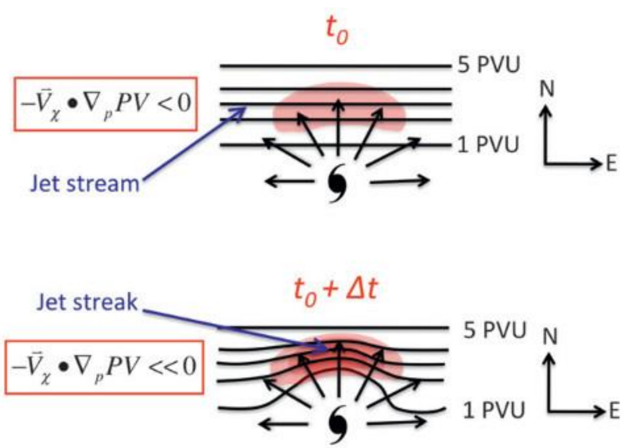

Archambault et al. (2013)

- Temporal evolution of tropopause-level flow can be evaluated by joint influence of **divergent** and **rotational** PV advection.

- Vertical advection and direct diabatic effect play a negligible role in upper troposphere.

Modification of midlatitude flows: Mechanisms

- **Local eddy kinetic energy (EKE) perspective** (Harr and Dea 2009; Quinting and Jones 2016; Keller 2017)

Baroclinic energy conversion

$$\frac{\partial K_e}{\partial t} = -\nabla(\mathbf{v}'\phi)_a - \omega\alpha - \frac{\partial(\omega\phi)}{\partial t} - \nabla(\mathbf{V}K_e) - \frac{\partial(\omega K_e)}{\partial p} - \mathbf{v}'\cdot(\mathbf{v}'\cdot\nabla\mathbf{V}_m) + \epsilon$$

Ageostrophic geopotential flux divergence (energy dispersion with group velocity)

Horizontal K_e flux divergence (K_e propagation with phase velocity)

where $\mathbf{V} = \mathbf{V}_m + \mathbf{v}'$

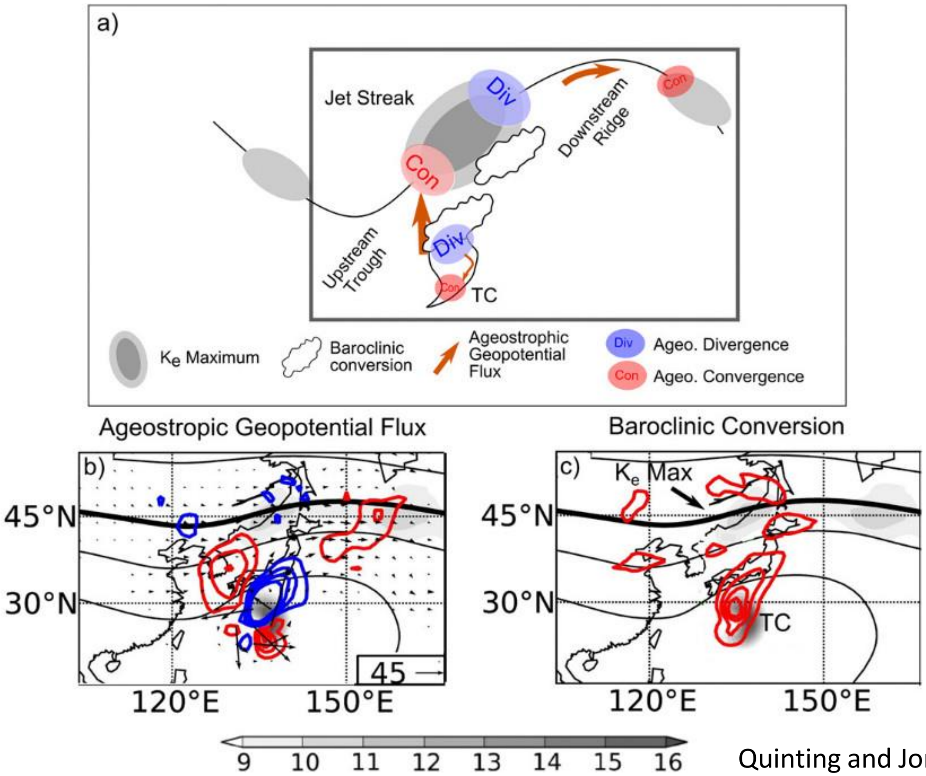

Quinting and Jones (2016)

- Rising warm moist air during ET releases K_e through the **baroclinic conversion**.
- This K_e is redistributed via ageostrophic geopotential flux divergence.
- Secondary cyclone in response to downstream development often act as another source of K_e.

Missing in the previous studies

- The **Structural changes of TCs** and **modification of midlatitude flow** during ET have been extensively studied [see Evans et al. (2017) and Keller et al. (2019) for comprehensive reviews].
- However, it is still unclear **how TC–midlatitude flow interaction modulates TC rainfall**. A few studies have been conducted on the landfalling hurricanes in eastern North America (e.g., Atallah and Bosart 2003; Atallah et al. 2007; Milrad et al. 2009), but such analyses are **still lacking in East Asia**.
- Some studies have addressed midlatitude preconditioning in East Asia (Byun and Lee 2012; Baek et al. 2015), but their analyses were confined to the indirect effects of TCs (i.e., predecessor rainfall events).

How does **midlatitude baroclinic condition** modulates the heavy rainfall events ***directly*** induced by TCs in South Korea?

TC–midlatitude flow interaction

Structure changes of TCs

Modification of midlatitude flow

?

Modulation of HREs

HRE: heavy rainfall event

Data & methods

Dataset (JJAS, 1979–2020)

- ERA5 reanalysis data (6 hourly, 1.5°x1.5°, 37 levels)
- Hourly precipitation records from weather stations in South Korea
- RSMC Tokyo-Typhoon Center TC best track

HREs (directly induced by TCs)

- 110 mm (12 h)$^{-1}$ at any single station
- Concurrence with TC in 32°–38°N, 120°–135°E ⍰ **A total of 68 events**

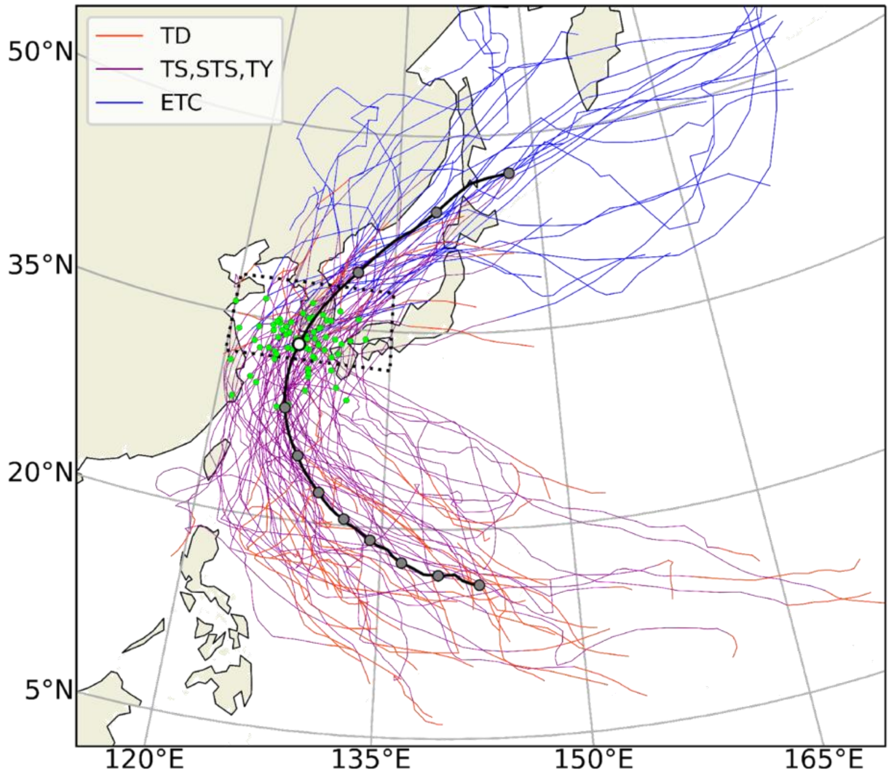

About 80% of TCs complete ET during or after HREs, continuing their lifecycle as extratropical cyclones.

TC locations in the mature stage of HREs (0 h)

Mean TC track (from -8 days to +3 days)

Tropopause-based self-organizing map (SOM) clustering

SOM Parameters	Selected option
Input data	Dynamic Tropopause (2-PVU height) at 30°–53°N & 105°–145°E at 0 h
Array of nodes	
Topology of node	Rectangular
Shape of map	Sheet
Initialization method	Linear initialization
Training method	Batch training
Neighborhood function	Epanechnikov function
Neighborhood radius	2 (initial), 1 (final)
Number of iterations	1,000 (rough training), 2,000 (fine tuning)

Why dynamic tropopause?

- The extent of TC–midlatitude flow interaction is known to be largely sensitive to midlatitude upper-level conditions.
- As an indicator of a waveguide for synoptic disturbances, it well captures not only the Rossby wave undulation but also the jet strength (deduced from its horizontal gradient) at the tropopause level, which represent the baroclinic environment.

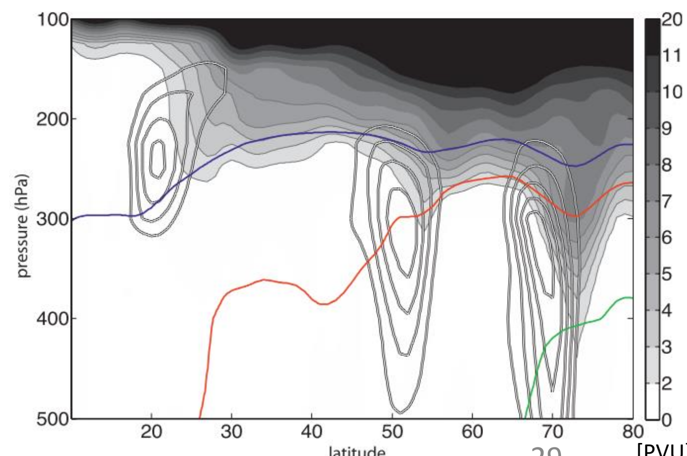

Martius et al. (2010)

Overview of two HRE clusters

Cluster 1 (58.8%) **Cluster 2** (41.2%)

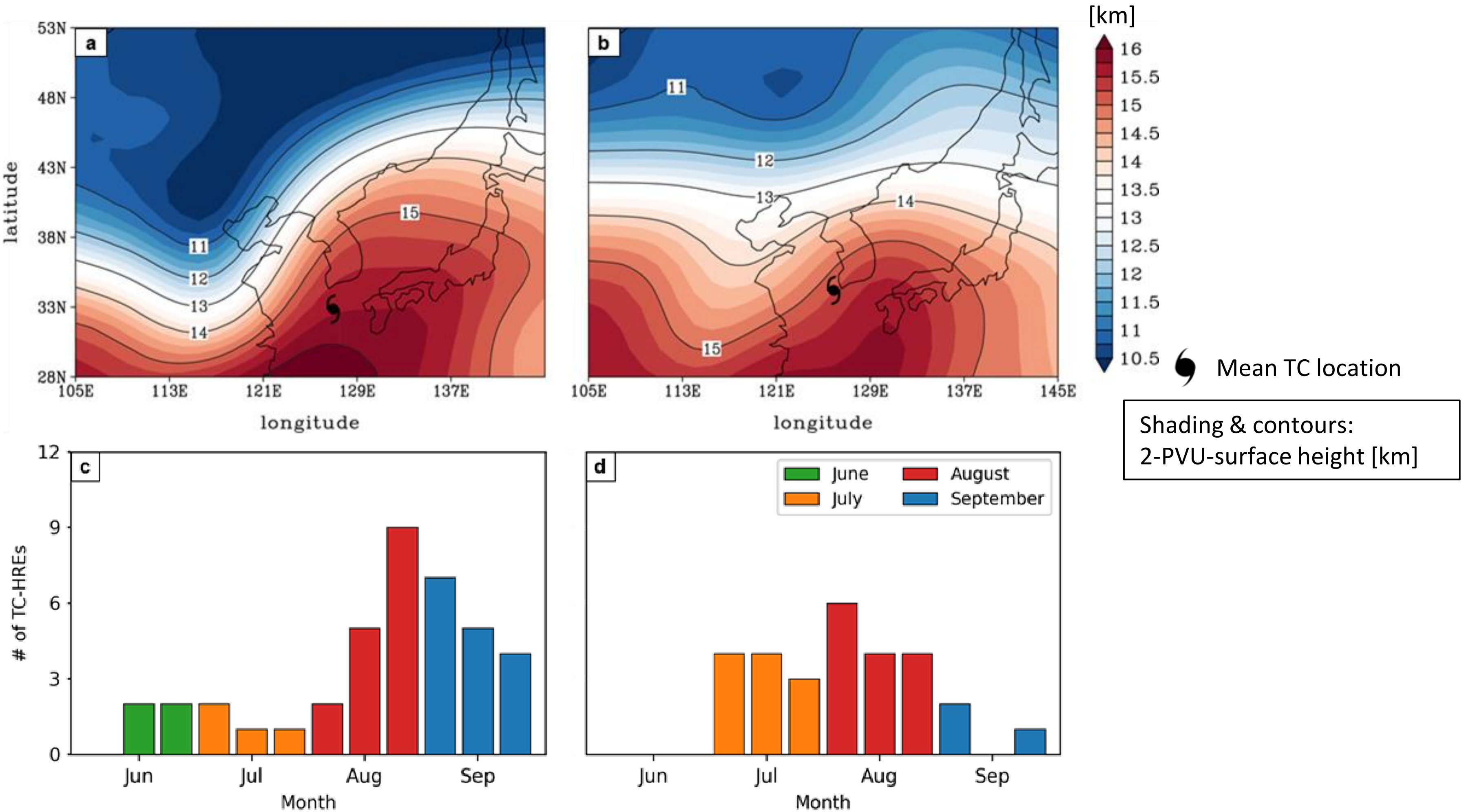

- Cluster 1: HREs under **strongly baroclinic** condition (late-summer type)
- Cluster 2: HREs under **weakly baroclinic** condition (mid-summer type)

Synoptic conditions: Tropopause (2-PVU surface)

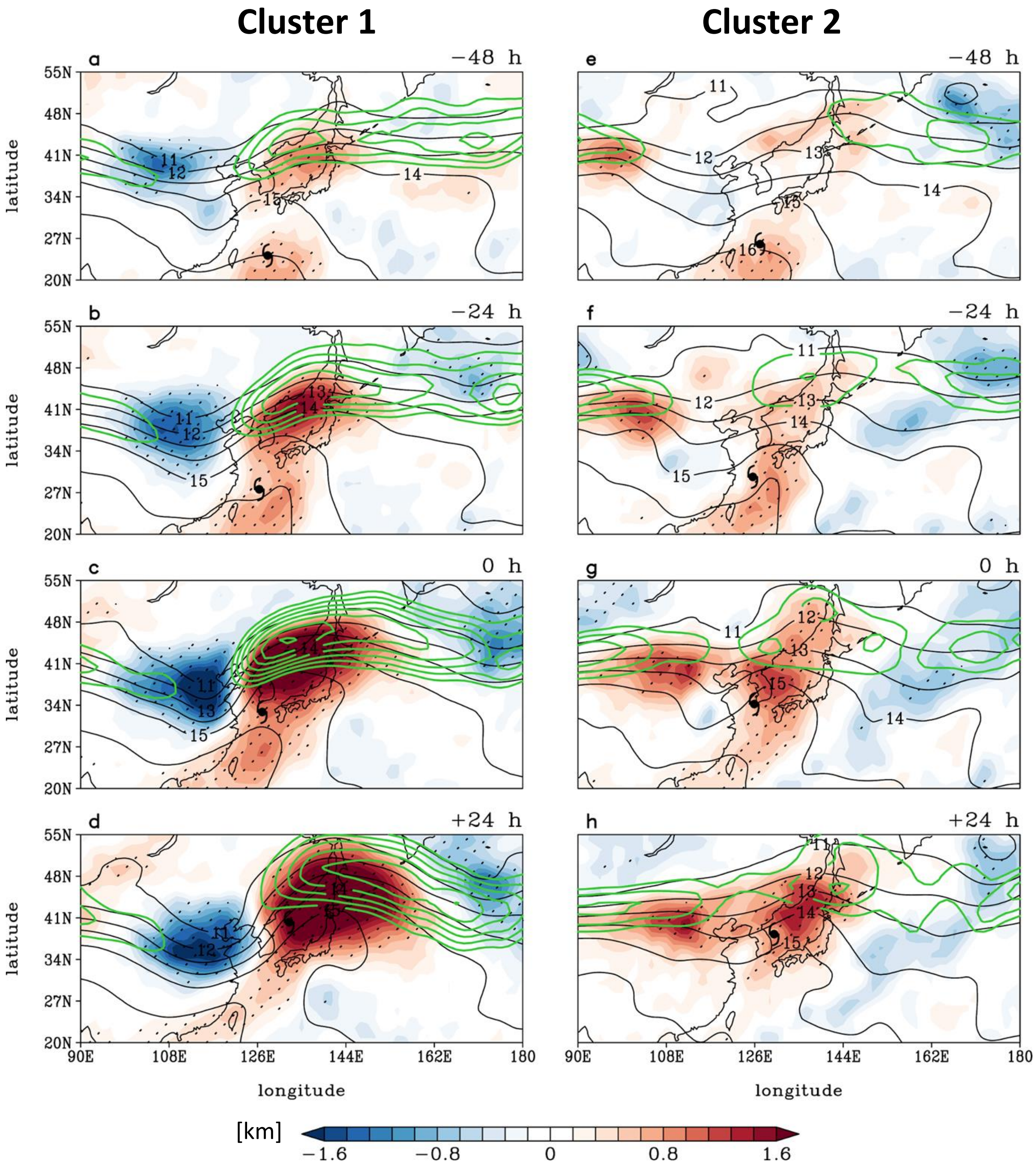

- C1 exhibits the amplifying trough-ridge couplet at tropopause, while C2 does not.

Mean TC location

Black contours: 2-PVU height [km]
Shading: 2-PVU height anomaly [km]
Green contours: : $|\mathbf{V}|$ at 2-PVU surface [m s^{-1}]

Synoptic conditions: Lower troposphere (700 hPa)

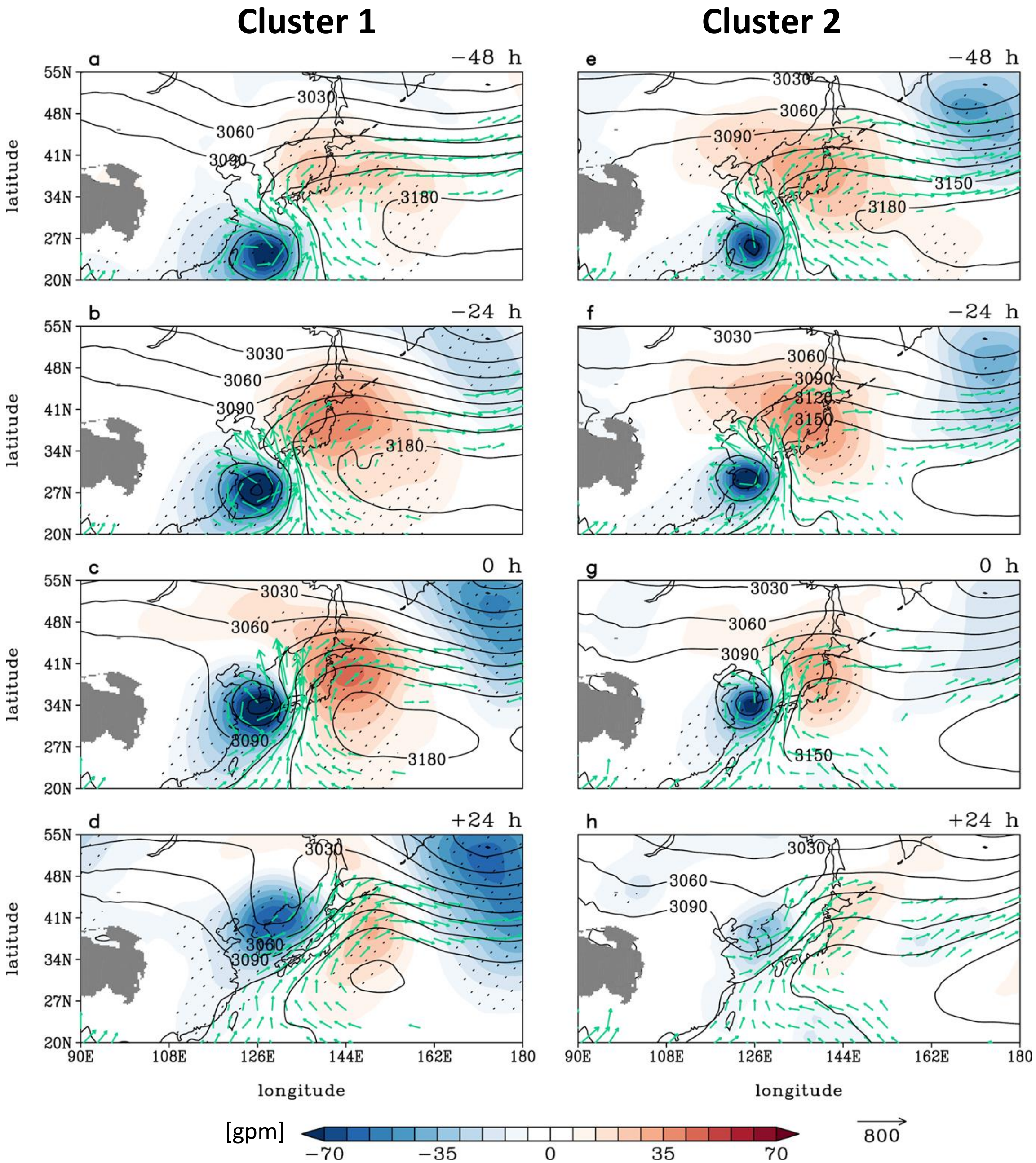

- C1 TCs sustain their size and intensity after HREs, while C2 TCs rapidly dissipate.

Contours: 700-hPa GPH [gpm]
Shading: 700-hPa GPH anomaly [gpm]
Vectors: **IVT** [> 300 kg m^{-1} s^{-1}]

Synoptic conditions: Lower troposphere (TC-centered)

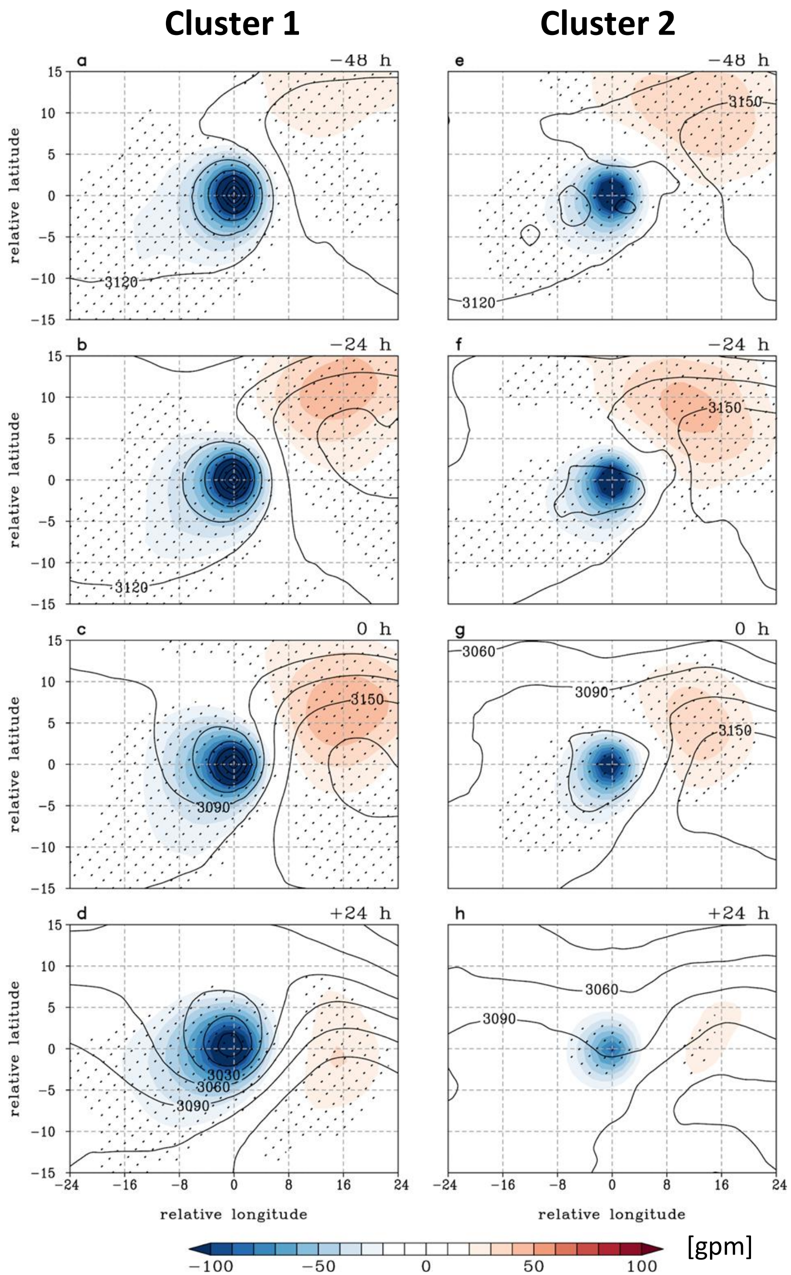

- The distinct TC evolution is not an artifact of composite analysis in which TC locations differ by events.

Contours: 700-hPa GPH [gpm]
Shading: 700-hPa GPH anomaly [gpm]

Cyclone phase space (CPS) diagram

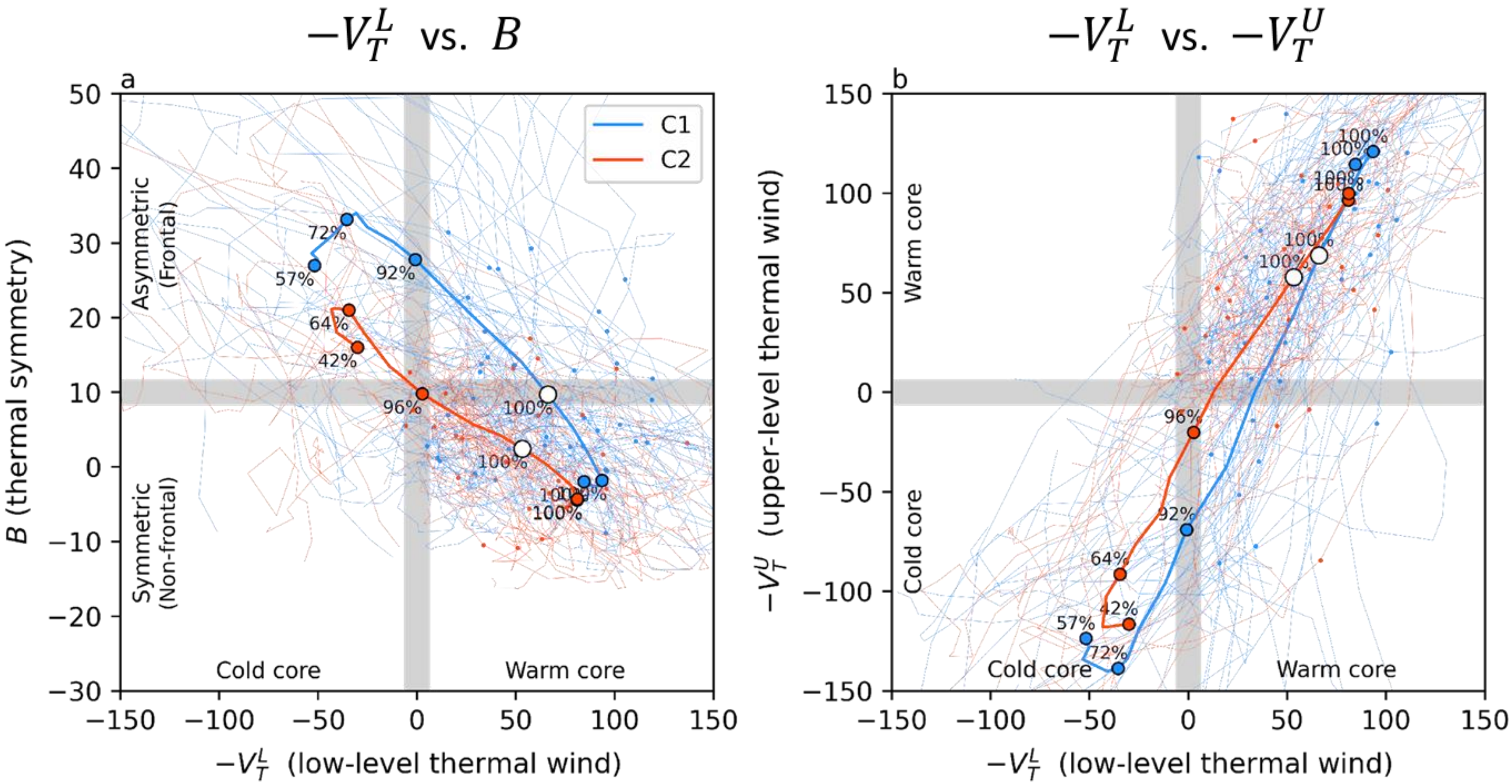

- C1 TCs exhibit the rapid development of thermal asymmetry and replacement of upper-level warm core by cold core, compared to C2 TCs.
- More than 90% of C1 TCs complete ET and continue their lifecycle as extratropical cyclones, whereas only about 60% of C2 TCs do so.

Synoptic conditions: lon-pres cross section (33°–39°N)

In the mature stage of HREs (0 h)

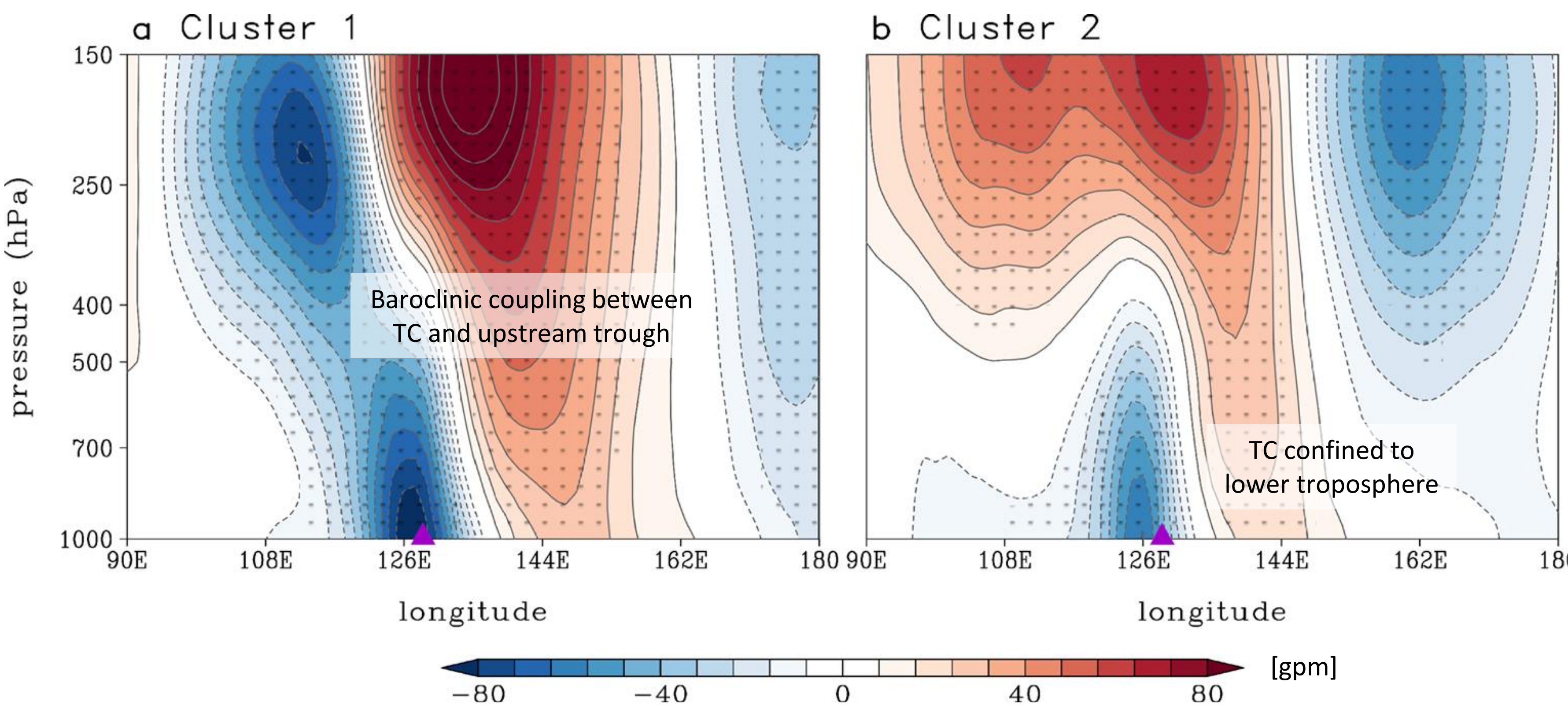

33°–39° N averaged
Shading: GPH anomaly [gpm]
Black contours: PV anomaly [PVU]

▲ South Korea

Synoptic conditions: lat-pres cross section (124°–131°E)

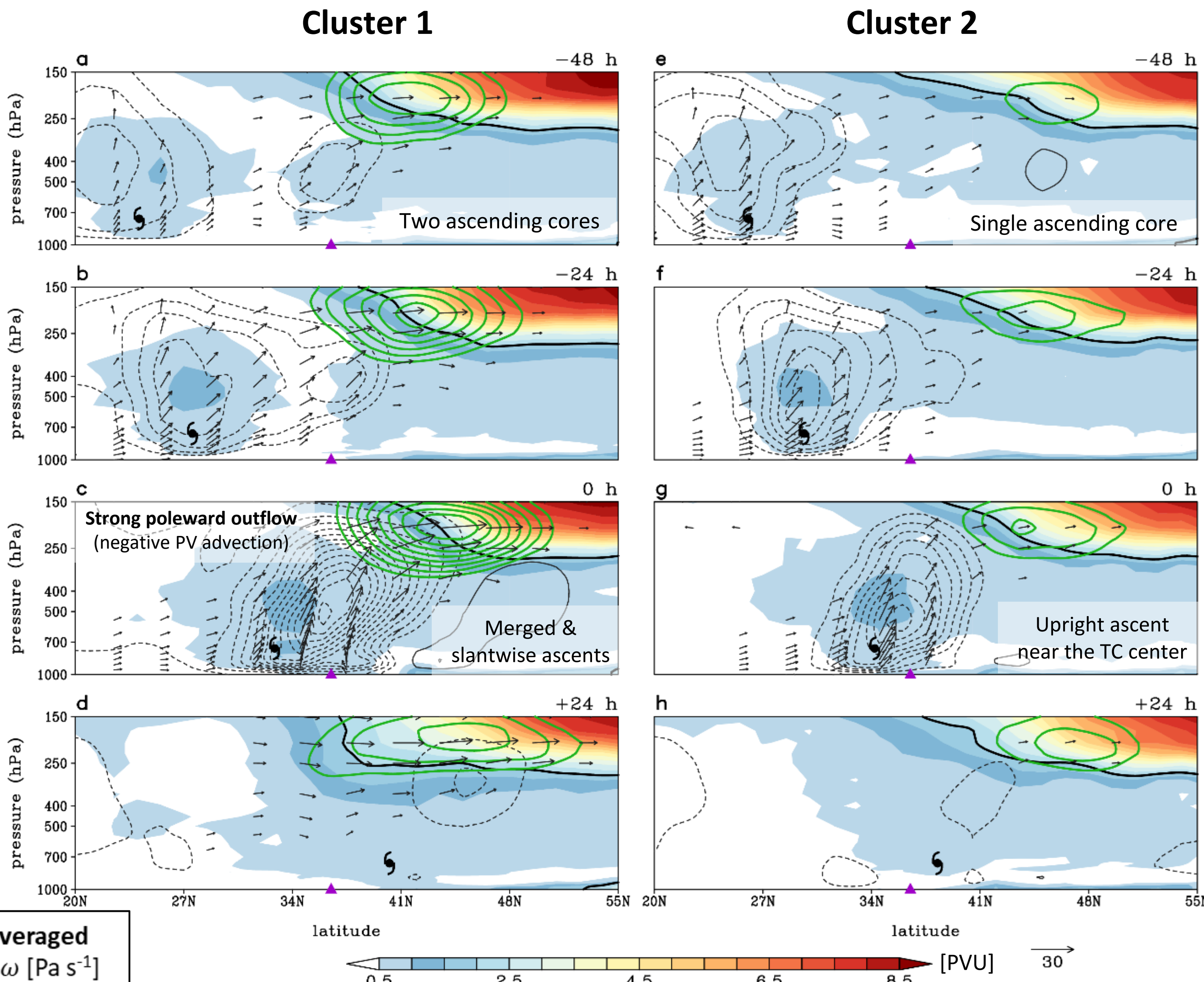

124°–131°E averaged
Black contours: ω [Pa s^{-1}]
Green contours: $|\mathbf{V}|$ [m s^{-1}]
Shading: PV [PVU]
Vectors: $v\omega$ [m s^{-1}]

▲ South Korea Mean TC location

Potential vorticity (PV) diagnosis of tropopause evolution

PV tendency equation

negligible　　negligible

$$\frac{\partial P}{\partial t} = -\mathbf{V}_\psi \cdot \nabla P - \mathbf{V}_\chi \cdot \nabla P - \cancel{\omega \frac{\partial P}{\partial p}} - g\left[(\zeta + f)\frac{\partial \dot{\theta}_{Dia}}{\partial p} \cancel{+ \frac{\partial \dot{\theta}_{Dia}}{\partial y}\frac{\partial u}{\partial p}} - \frac{\partial \dot{\theta}_{Dia}}{\partial x}\frac{\partial v}{\partial p}\right]$$

Advection by rotational wind | Advection by divergent wind | Vertical advection | Diabatic production

* 250–150-hPa layer average is applied

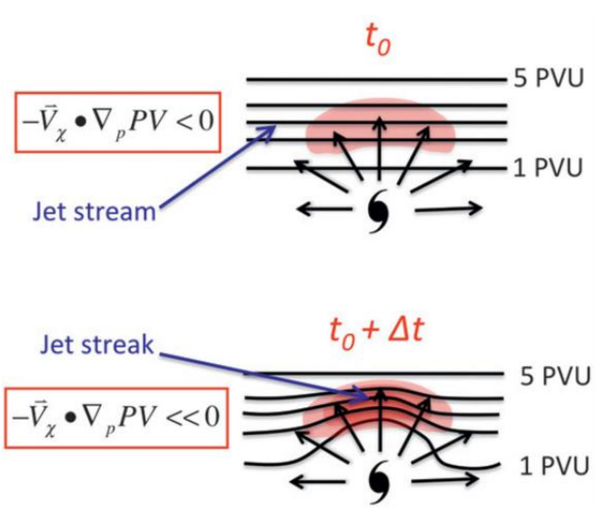

Archambault et al. (2013)

At mature stage of HREs (0 h)

Cluster 1　　**Cluster 2**

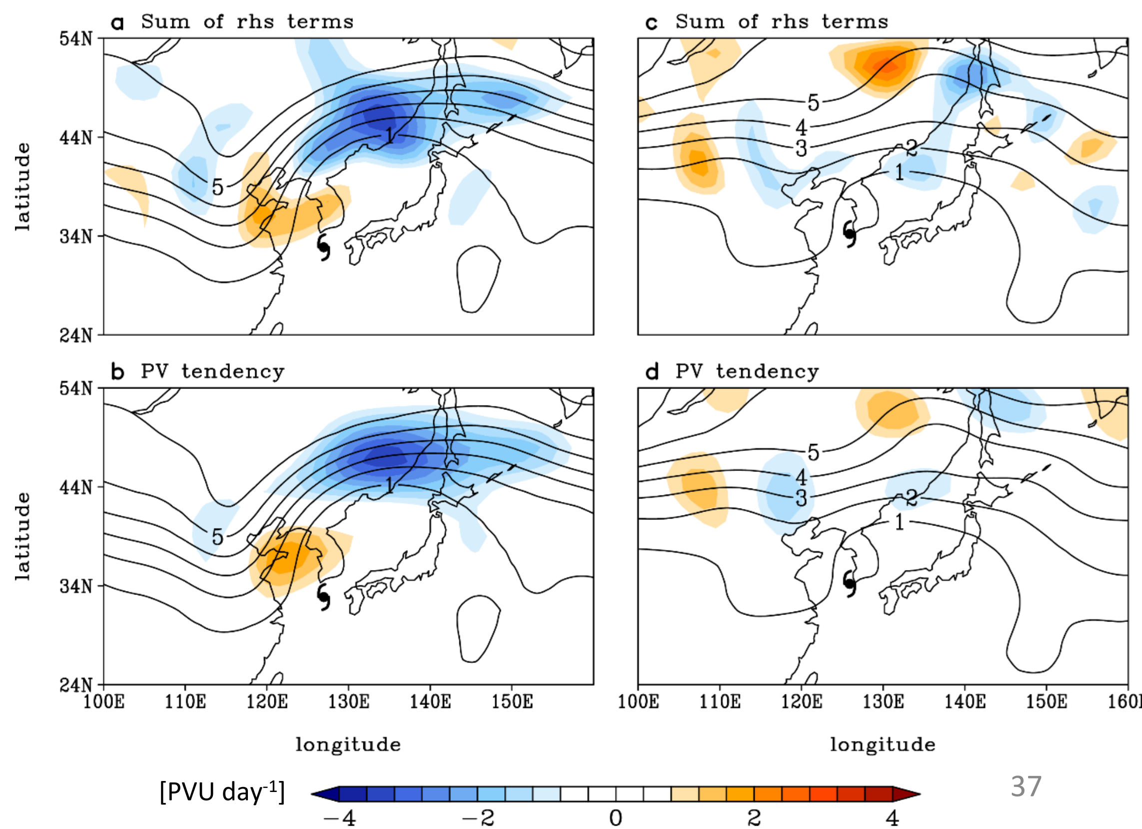

Potential vorticity (PV) diagnosis of tropopause evolution

At mature stage of HREs (0 h)

$$\frac{\partial P}{\partial t}$$

$$-\mathbf{V}_{\psi} \cdot \nabla P$$

(mostly, by midlatitude flow)

$$-\mathbf{V}_{\chi} \cdot \nabla P$$

(mostly, by TC outflow)

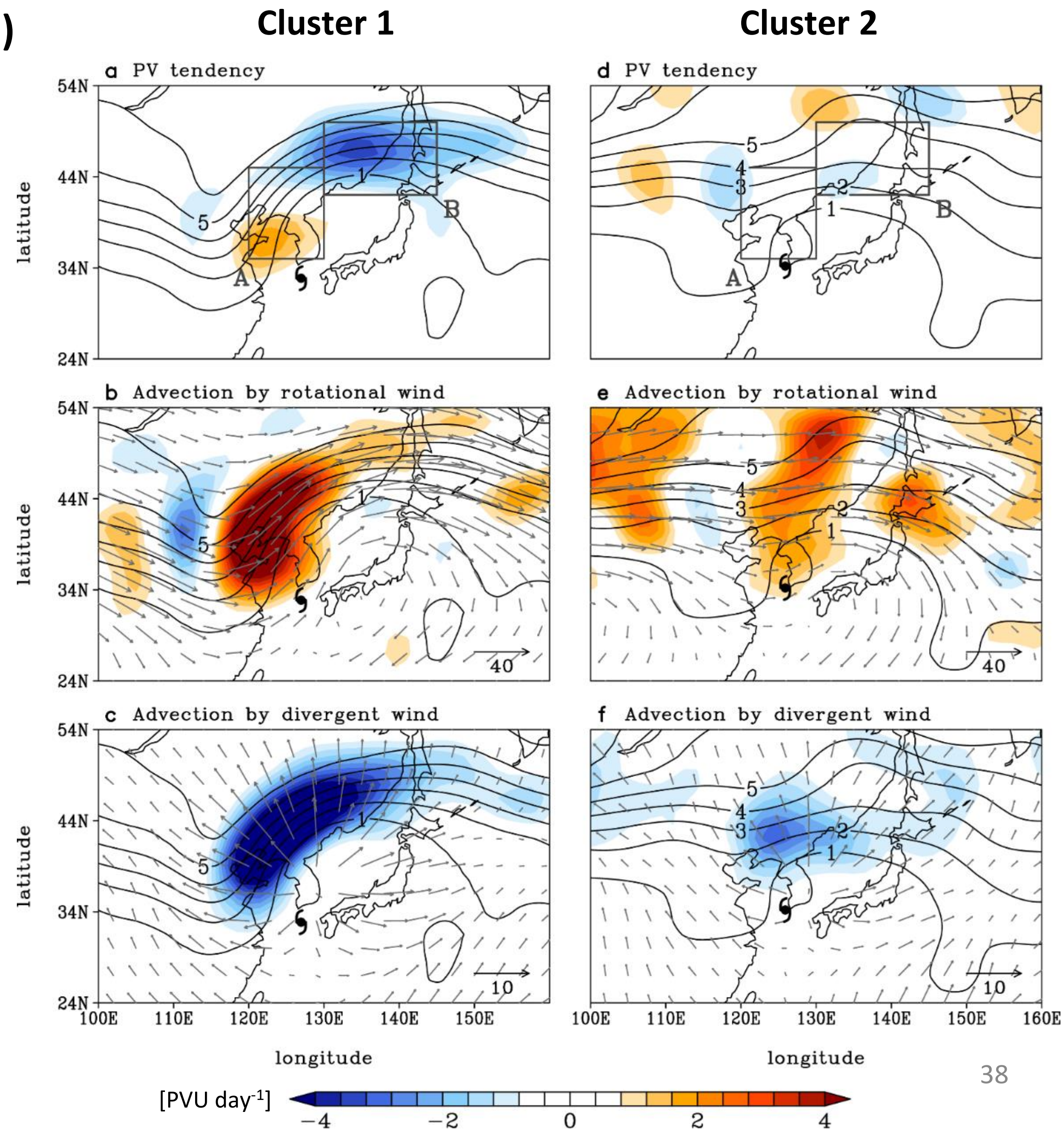

250–150-hPa average
Shading: PV budget term [PVU day^{-1}]
Black contours: PV [PVU]

Quasi-geostrophic (QG) diagnosis of vertical motion

Dynamic forcing (ω_{Dyn})

negligible in
synoptic-scale motion

$$\left(\sigma_0 \nabla^2 + f_0^2 \frac{\partial^2}{\partial p^2}\right)\omega = \boxed{-2\nabla \cdot Q_n \mathbf{n} - 2\nabla \cdot Q_s \mathbf{s}} + \cancel{f_0 \beta_0 \frac{\partial v_g}{\partial p}} - \frac{\kappa}{p}\nabla^2 J$$

Transverse
Q-vector forcing (ω_n)

Shearwise
Q-vector forcing (ω_s)

Beta forcing (ω_{Beta})

Diabatic forcing (ω_{Dia})

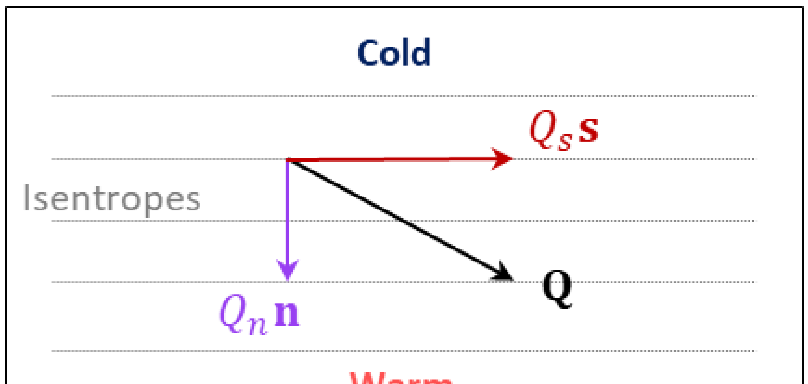

Keyser et al. (1988; 1992)

$Q_s\mathbf{s}$: Shearwise Q vector

- Lagrangian change of $\nabla\theta$ direction following the geostrophic motion
- Trough/ridge, isolated vortex (e.g., TC)

$Q_n\mathbf{n}$: Transverse Q vector

- Lagrangian change of $\nabla\theta$ magnitude following the geostrophic motion
- Confluent/diffluent flows (e.g., jet entrance)

Quasi-geostrophic (QG) diagnosis of vertical motion

Cluster 1

At mature stage of HREs (0 h)

Ascending ω_s by upper-level trough and ridge

Elongated ascending ω_n by confluent motion around the jet entrance (secondary circulation)

Black contours: GPH [gpm]
Shading: ω_s [Pa s^{-1}]
Vectors: $Q_s\mathbf{s}$ [10^{-12} m^2 kg s^{-1}]

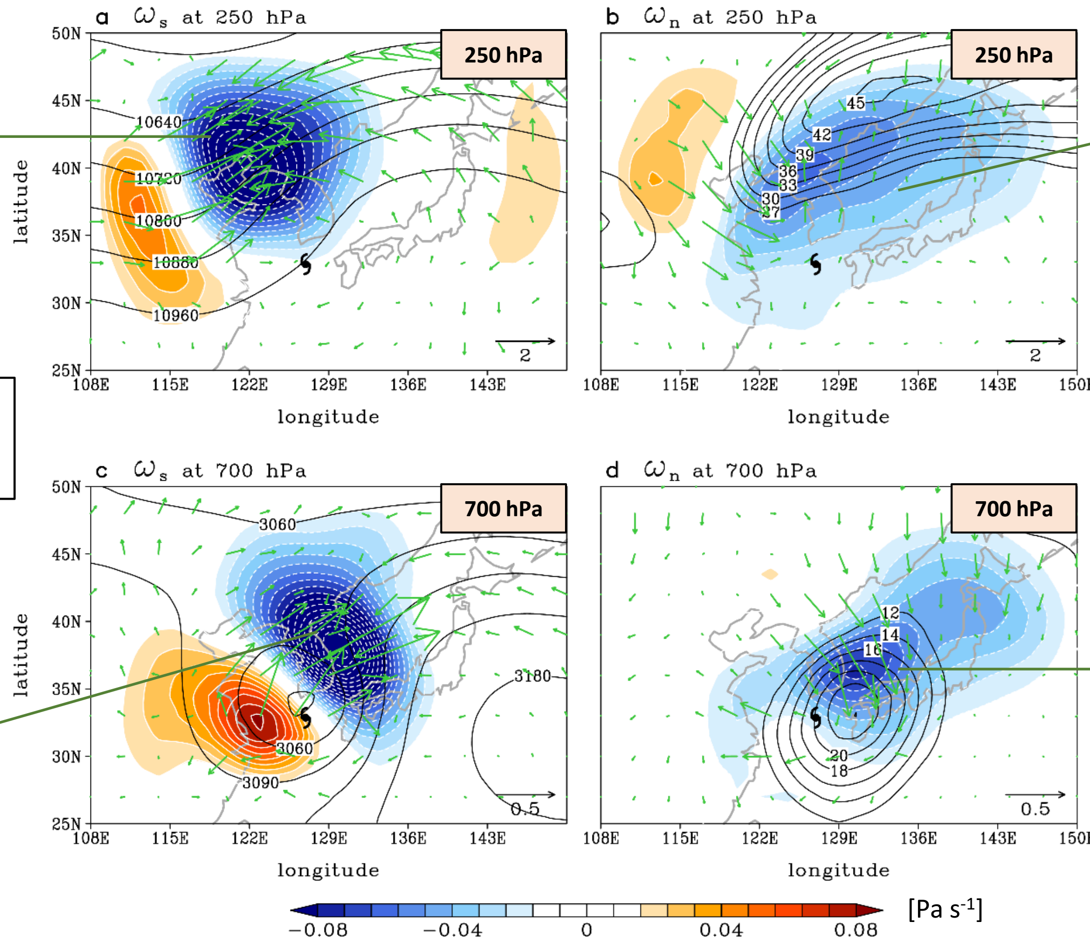

Black contours: $|\mathbf{V}|$ [m s^{-1}]
Shading: ω_n [Pa s^{-1}]
Vectors: $Q_n\mathbf{n}$ [10^{-12} m^2 kg s^{-1}]

Ascending ω_s by TC-induced rotating flow

Elongated ascending ω_n by southerly TC flow (warm front development)

- Widely-enhanced ω_{Dyn} ($= \omega_n + \omega_s$) is associated with various dynamical processes manifesting synergistic TC–midlatitude flow interaction.

Quasi-geostrophic (QG) diagnosis of vertical motion

Cluster 2

At mature stage of HREs (0 h)

Black contours: GPH [gpm]
Shading: ω_s [Pa s^{-1}]
Vectors: $Q_s \mathbf{s}$ [10^{-12} m^2 kg s^{-1}]

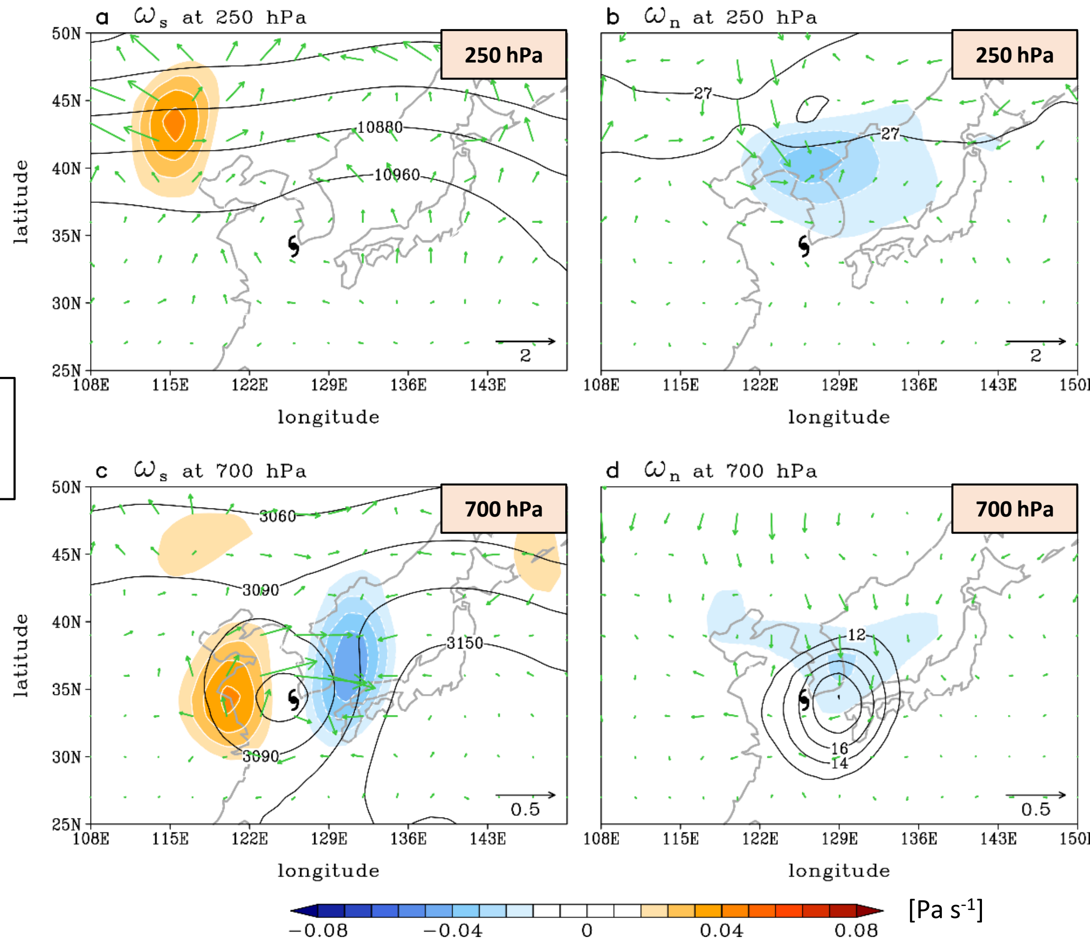

Black contours: $|\mathbf{V}|$ [m s^{-1}]
Shading: ω_n [Pa s^{-1}]
Vectors: $Q_n \mathbf{n}$ [10^{-12} m^2 kg s^{-1}]

- The dynamic ascent is feeble in both the upper and lower troposphere.

Quasi-geostrophic (QG) diagnosis of vertical motion

At 500 hPa

Cluster 1

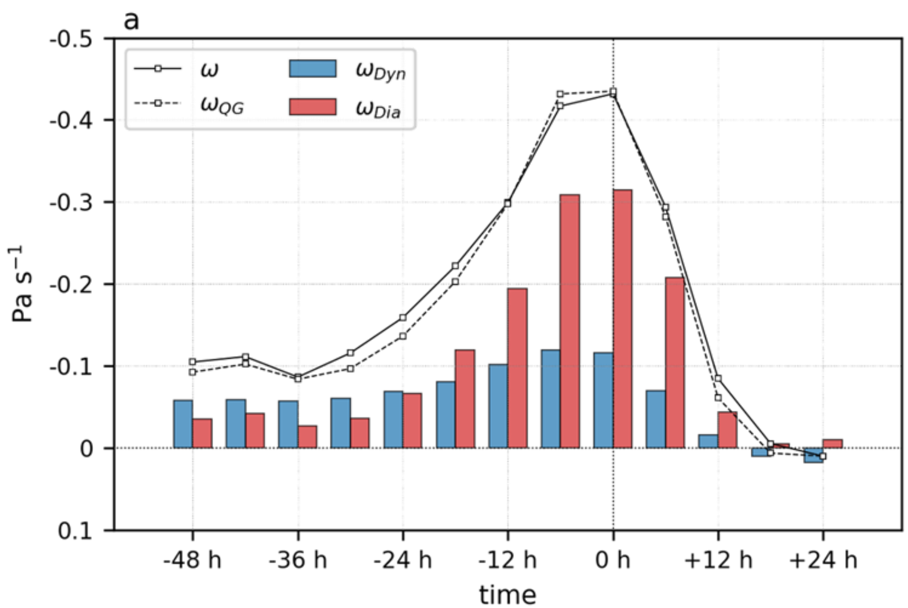

Cluster 2

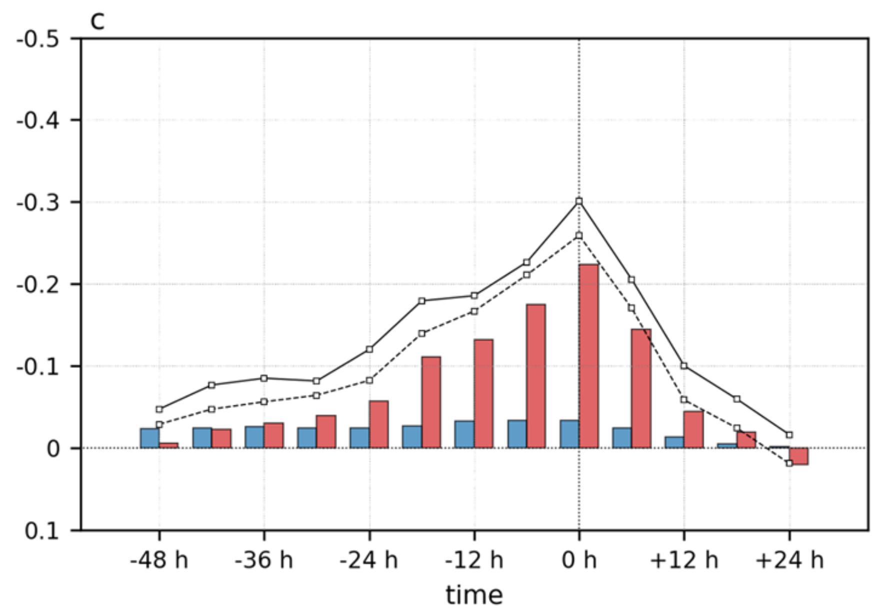

- C1 HREs is characterized by the nonlinear feedback of ω_{Dyn} and ω_{Dia} fostered by TC–midlatitude flow interaction.
- C2 HREs are dominated by ω_{Dia} with negligible ω_{Dia}, implying the dominant role of inherent diabatic TC convection.

Comparison of TC rainfall distribution (TC-centered composite)

ERA5 12-h accumulated ERA5 total precipitation at 0 h

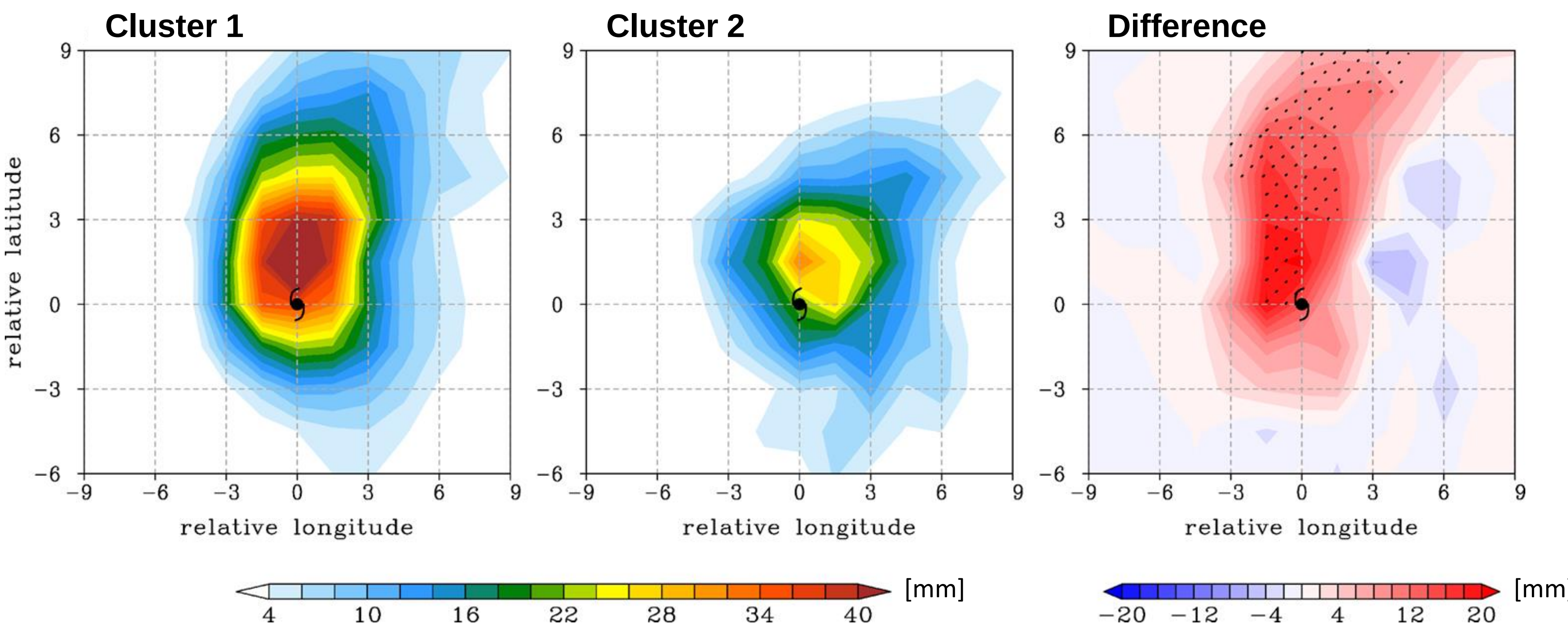

- TC rainfall is largely enhanced to the north of TC center in C1, whereas rainfall is relatively confined to TC center in C2.
- This is consistent with the **widely enhanced ω_{Dyn} in C1** and the **weak and spatially limited ω_{Dyn} in C2**.

Comparison of TC rainfall distribution (South Korea)

Maximum 12-h accumulated rainfall across 57 stations

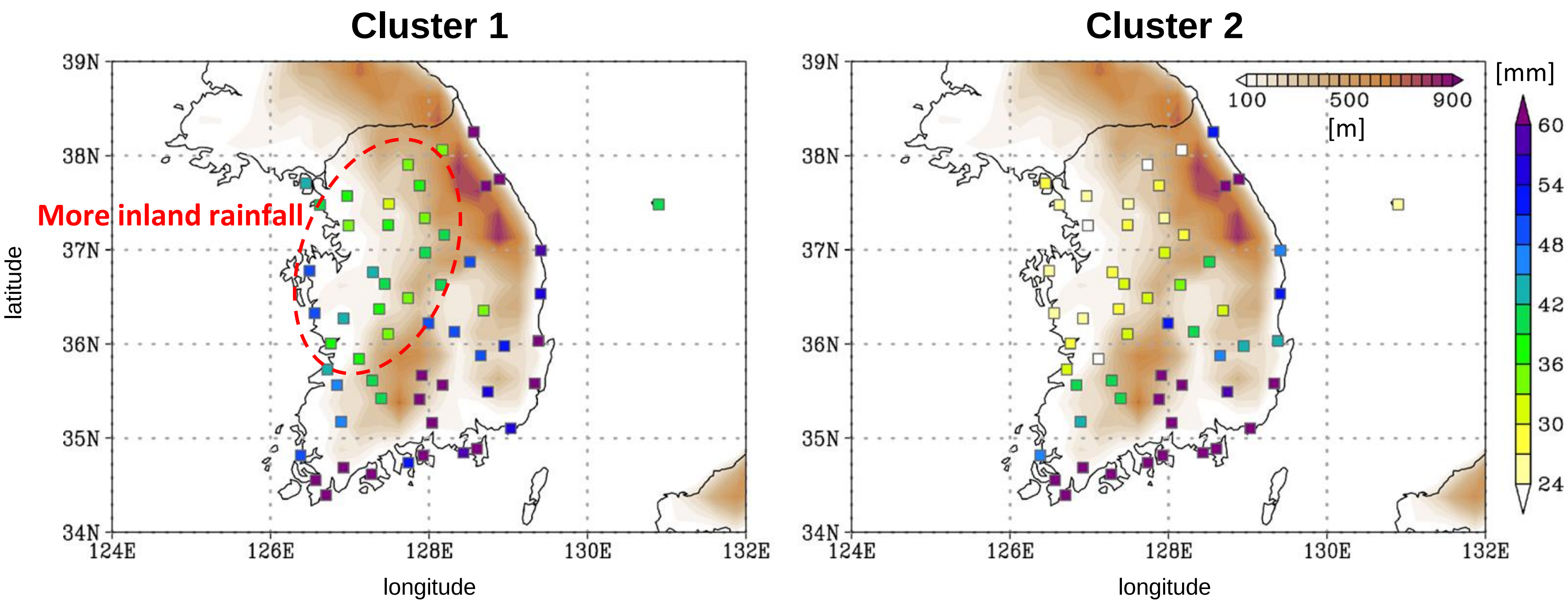

- C1 HREs bring more inland rainfall than C2 HREs (i.e., nationwide impact).
- This is consistent with the widely enhanced ω_{Dyn} in C1 and the weak and spatially limited ω_{Dyn} in C2.

Comparison of TC tracks

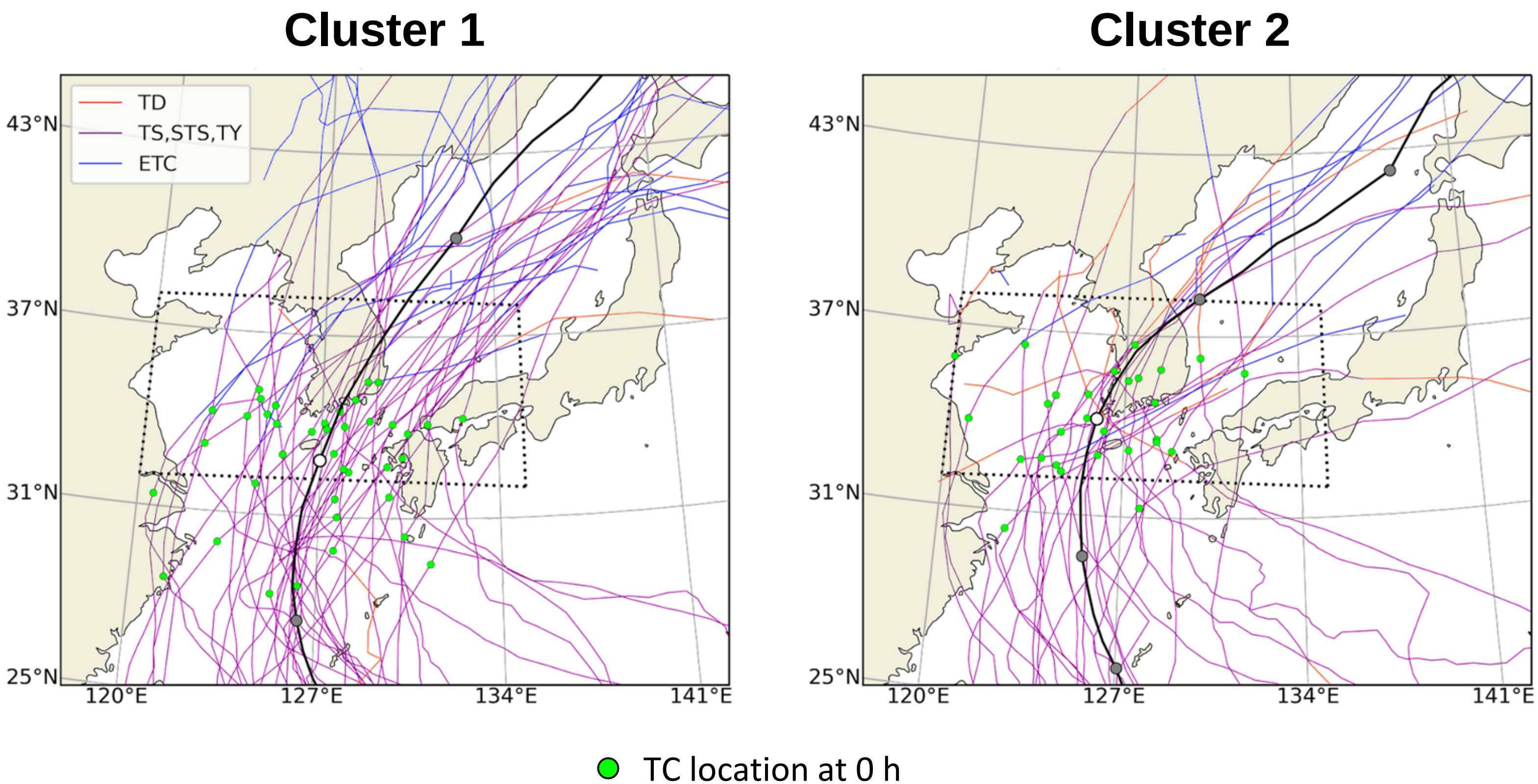

- Unlike C2 HREs, C1 HREs are in the mature stage even before landfalling.
- This is consistent with the widely enhanced ω_{Dyn} in C1 and the weak and spatially limited ω_{Dyn} in C2.

Representative case: Hinnamnor (2022)

Cyclone phase space diagram

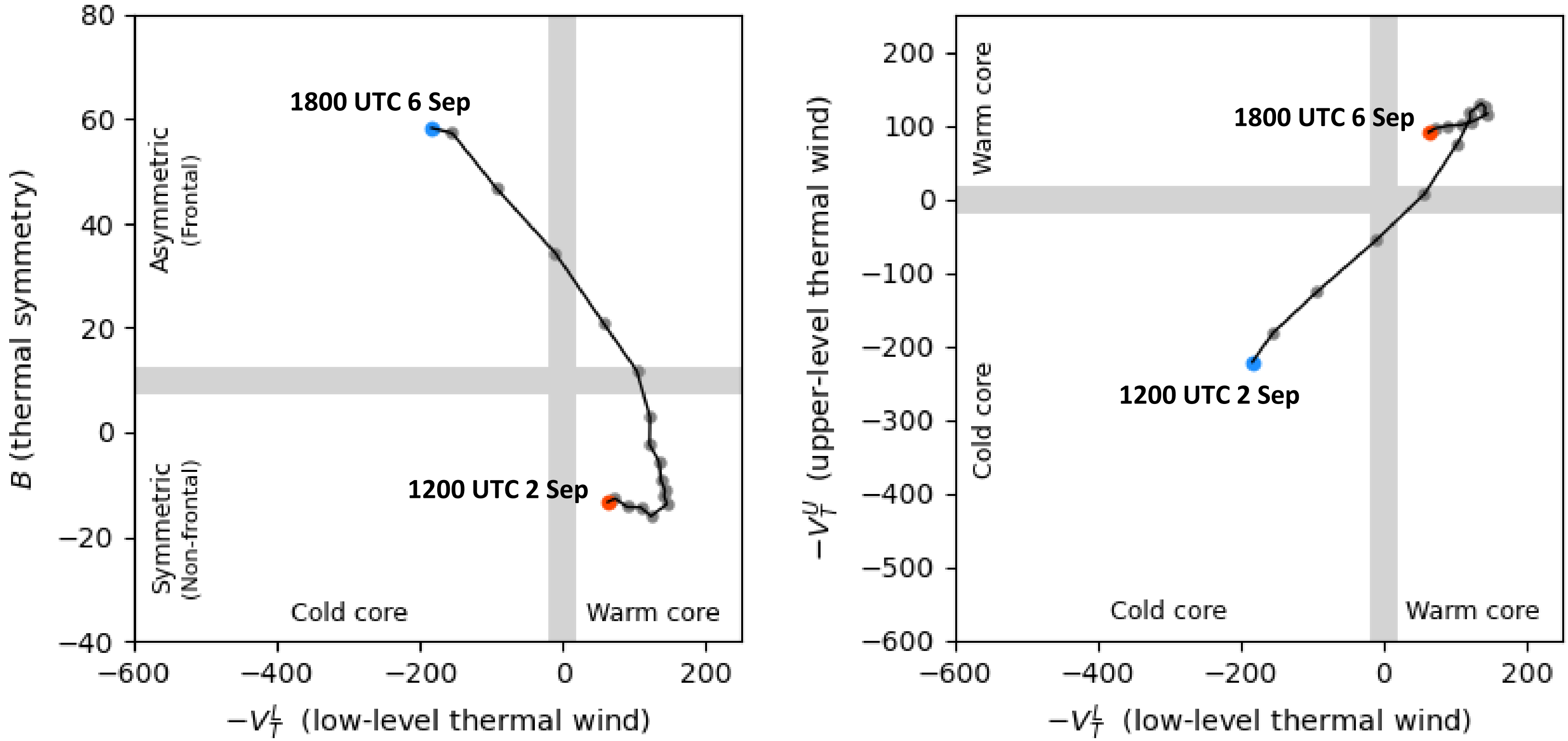

- Hinnamnor (2022) strongly interacted with midlatitude flow, following the typical evolution path of ET in the western North Pacific.

Representative case: Hinnamnor (2022)

1910 KST 5 September

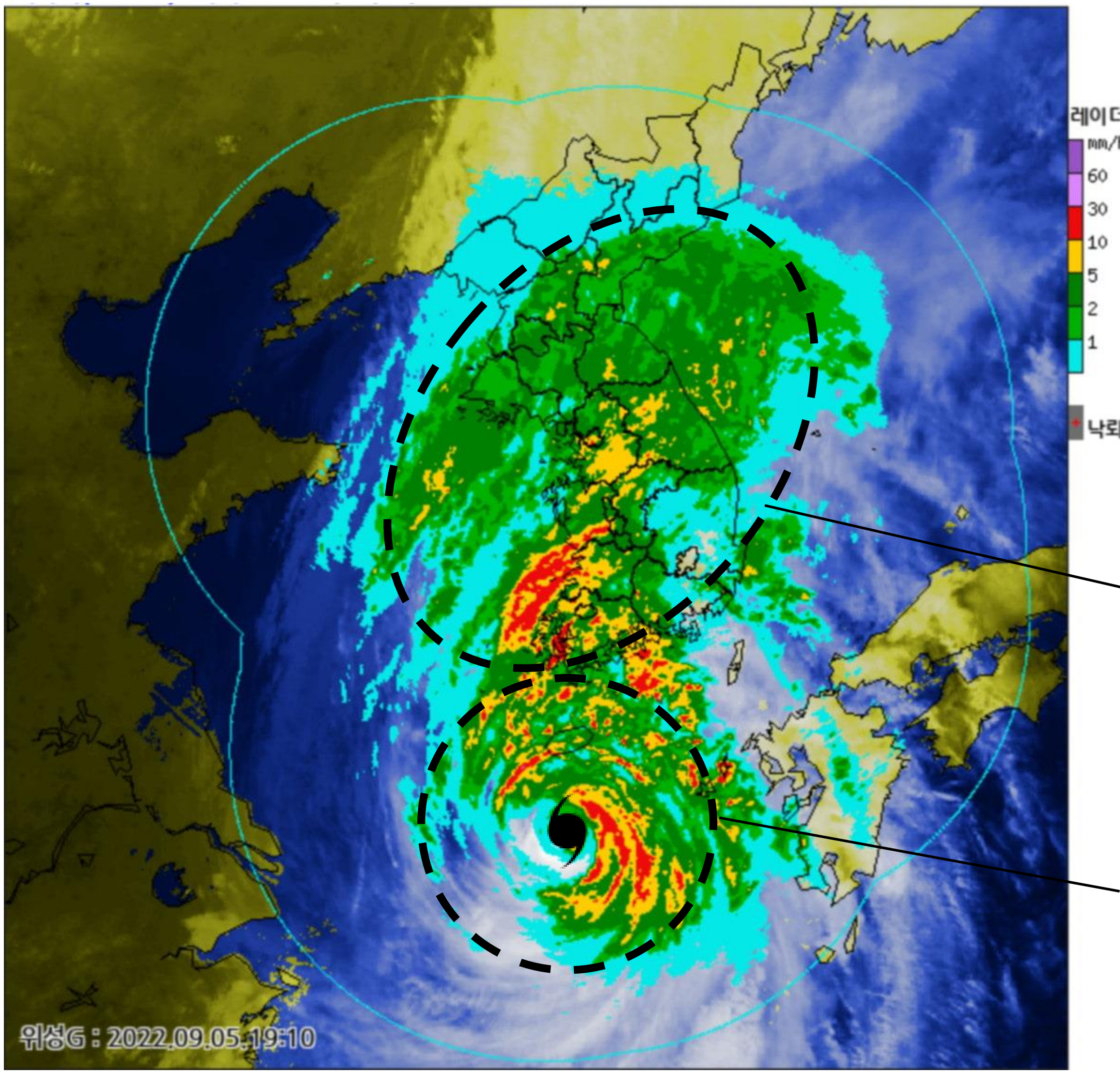

TC-ahead rain shield
(TC–midlatitude flow interaction)

Spiral rainband
(inherent TC convection)

Summary

- C1: HREs under **strongly baroclinic** condition (58.8%)
  - Late-summer prevalence
  - Quasi-stationary trough-ridge couplet
  - Phase locking of TCs with upstream trough
  - Significant structural changes of TCs

"Synergistic"
TC-midlatitude flow interaction

Widely enhanced QG dynamic uplift →
✓ Widespread rainfall to the north of TC center
✓ HREs even prior to TC landfall

- C2: HREs under **weakly baroclinic** condition (41.2%)
  - Mid-summer prevalence
  - Unamplified tropopause pattern
  - Rapid TC dissipation
  - Maintenance of tropical features of TCs

"Weak"
TC-midlatitude flow interaction

Vertical motion confined to inherent TC convection →
✓ Narrow rainfall area near the TC center
✓ HREs during TC landfall

Summary

How does **midlatitude baroclinic condition** modulates the heavy rainfall events ***directly*** induced by TCs in South Korea?

TC–midlatitude flow interaction

Structure changes of TCs

Modification of midlatitude flow

?

Modulation of HREs

HRE: heavy rainfall event

- Midlatitude baroclinic condition plays a critical role in the strength of TC–midlatitude flow interaction and thereby determines the spatial extent of tropical cyclone rainfall.
- Thus, midlatitude environment should be carefully considered as a factor of heavy rainfall events directly induced by tropical cyclones.
- These results may be also applied to neighboring countries (e.g., China, Japan).

Thank you for listening!

Park, C., S.-W. Son*, Y. N. Takayabu, S.-H. Park, D.-H. Cha, and E.-J. Cha: **Role of midlatitude baroclinic condition in heavy rainfall events directly resulting from tropical cyclones in South Korea**. *Mon. Wea. Rev.*, in revision.

Contact: chanil0602@snu.ac.kr
Homepage: https://sites.google.com/view/chanil-weather

Back-up slides

Sensitivity to TC intensity prior to entering baroclinic zone

Lifetime minimum central pressure

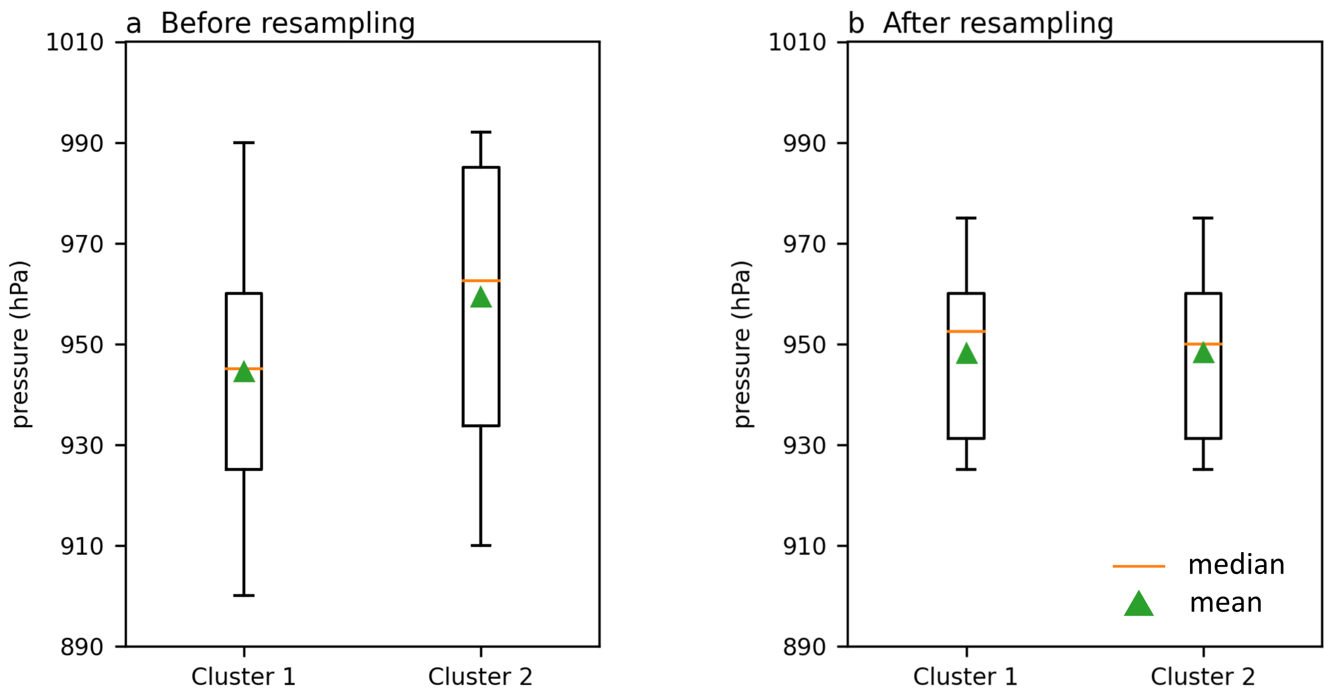

- C1 TCs more strongly develop before entering midlatitude baroclinic zone.
- TCs are resampled so that those in C1 and C2 have similar lifetime minimum central pressure (30 and 14 events in C1 and C2, respectively).

The essentially same results are obtained with the resampled HREs (figure not shown)!

C1 HREs *vs.* predecessor rainfall events (PREs)

36-h accumulated precipitation

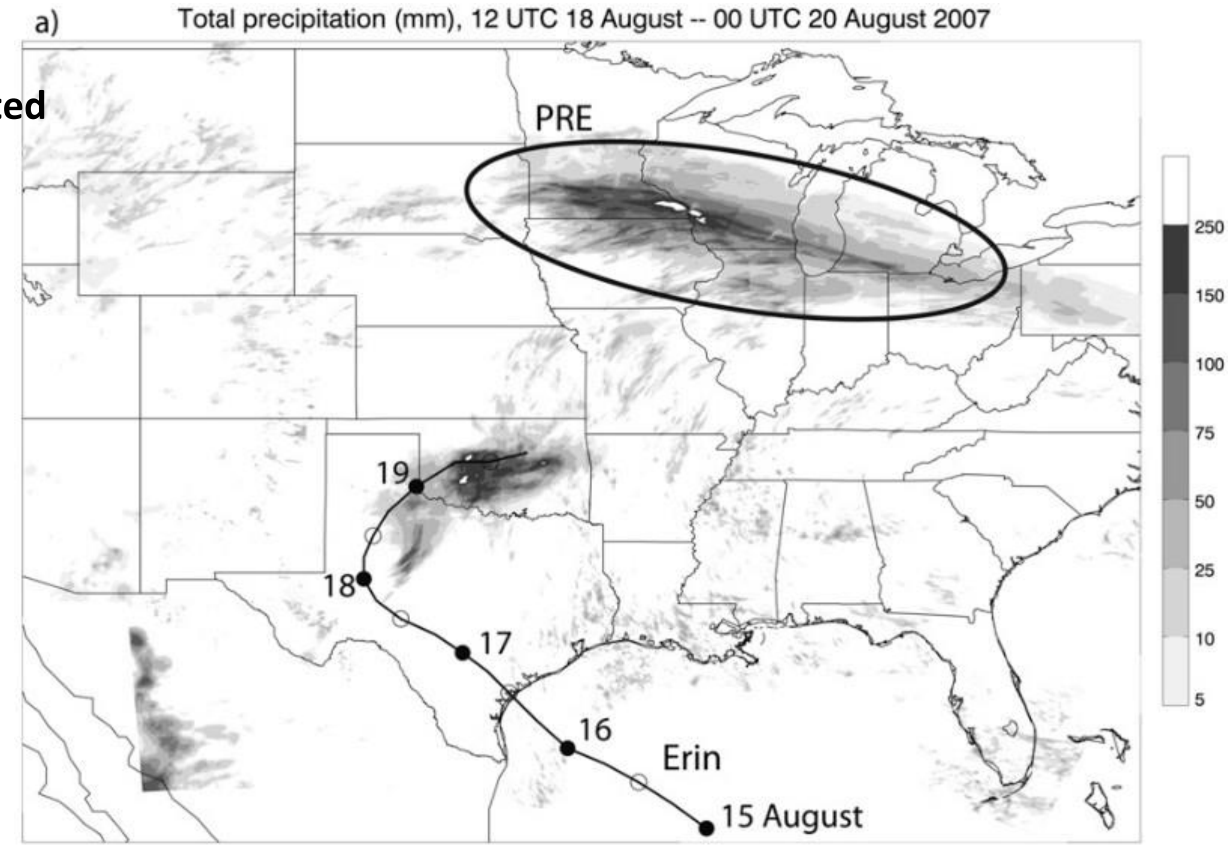

Schumacher and Galarneau (2012)

- PREs are clearly separated from TC rainfall (distance > 1000 km).
- PREs occur when the remotely-supplied moisture is lifted by the purely midlatitude processes.

Statistical relationship bwt Rainfall Area & VWS (Kim et al. 2019)

PLOS | ONE

RESEARCH ARTICLE

Influence of vertical wind shear on wind- and rainfall areas of tropical cyclones making landfall over South Korea

Dasol Kim[1], Chang-Hoi Ho[1]*, Doo-Sun R. Park[2]

1 School of Earth and Environmental Sciences, Seoul Natio
2 Department of Earth Sciences, Chosun University, Gwan
Meteorological Sciences, Korea Meteorological Administrati

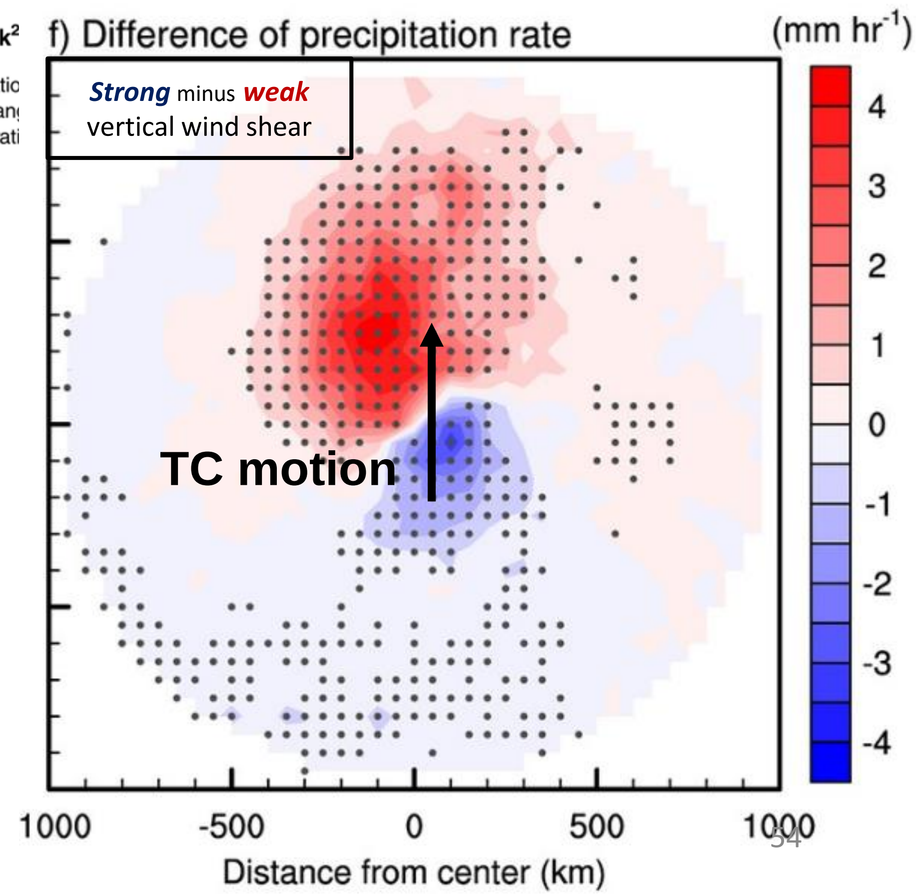

Our result dynamically supports the statistical findings of Kim et al. (2019).

Inertial stability

A measure of the resistance to radial motion

$$I^2 = (f + 2\,v_t/r)(f + \zeta)$$

v_t: tangential wind (positive for counterclockwise)

r: radial distance from the TC center

f: planetary vorticity

ζ: vertical component of relative vorticity

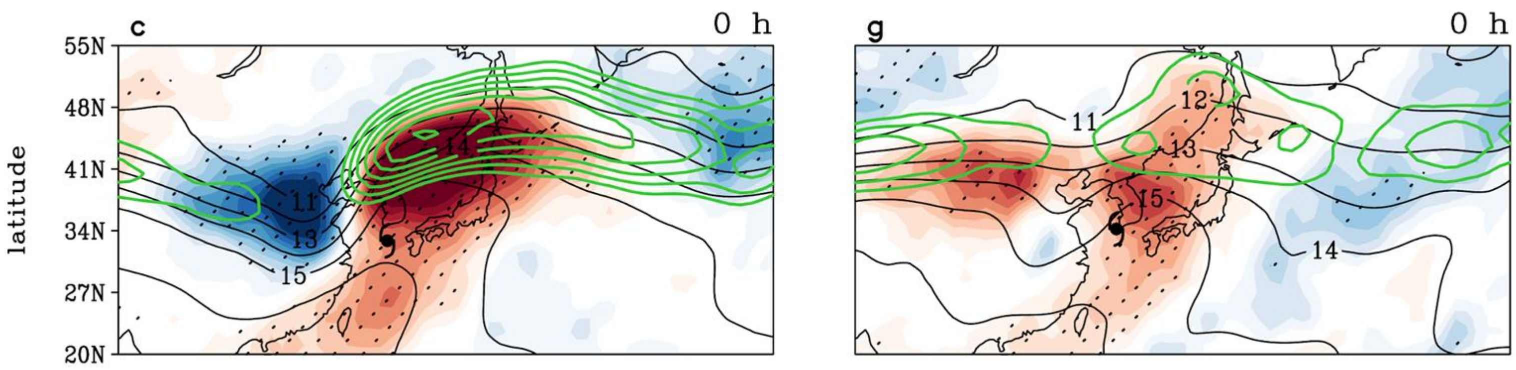

In C1, the upper-level jet to the north of TCs and deepened trough to the west of TCs locally reduce v_t, ζ, and thereby I^2.

Time evolution of PV tendency budget

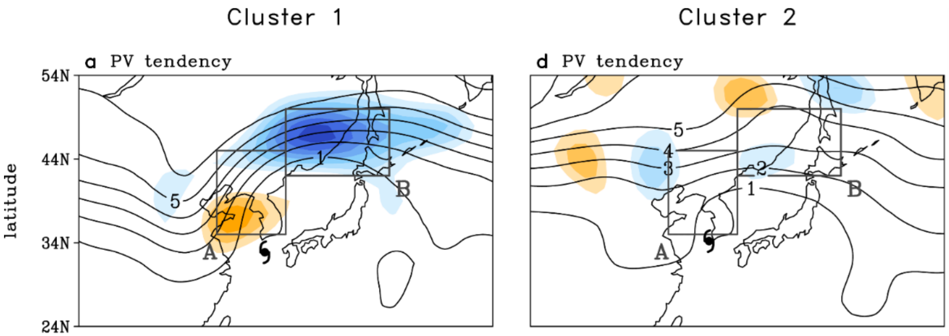

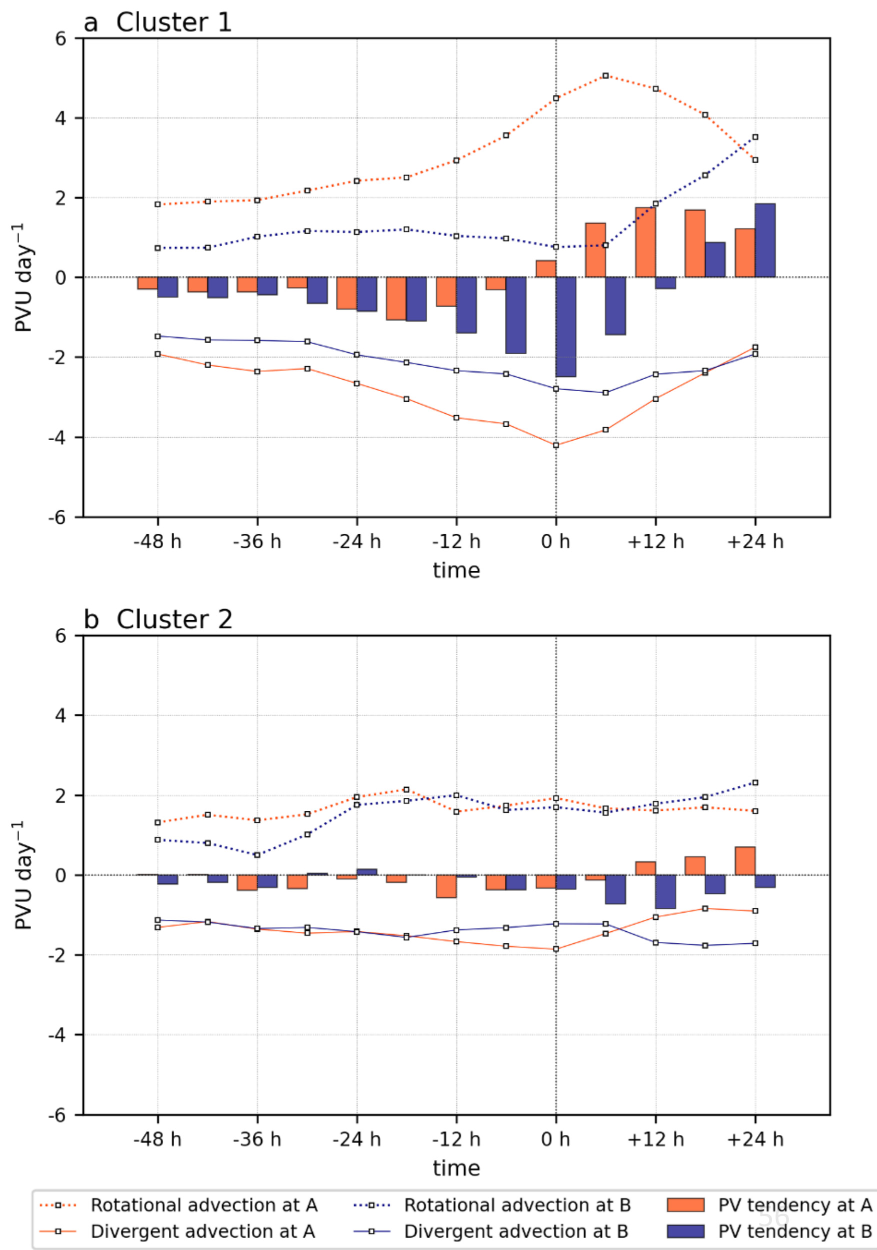

List of events

Cluster 1 (58.8%)			Cluster 2 (41.2%)		
Num	HRE reference time [UTC]	TC name, ID	Num	HRE reference time [UTC]	TC name, ID
1	1979.08.17.00	Irving, 7910	1	1979.08.24.17	Judy, 7911
2	1980.09.10.18	Orchid, 8013	2	1981.07.31.17	Ogden, 8110
3	1984.08.20.21	Holly, 8410	3	1981.09.02.09	Agnes, 8118
4	1985.08.13.20	Lee, 8509	4	1982.08.13.16	Cecil, 8211
5	1985.08.31.08	Odessa, 8512	5	1982.08.27.04	Ellis, 8213
6	1986.06.24.10	Nancy, 8605	6	1985.08.10.08	Kit, 8508
7	1986.08.27.20	Vera, 8613	7	1990.07.11.07	Robyn, 9007
8	1987.07.15.11	Thelma, 8705	8	1991.08.23.02	Gladys, 9112
9	1987.08.30.17	Dinah, 8712	9	1994.08.01.07	Brendan, 9411
10	1989.07.28.13	Judy, 8911	10	1994.08.10.01	Doug, 9413
11	1990.09.01.00	Abe, 9015	11	1995.07.23.10	Faye, 9503
12	1991.09.27.02	Mireille, 9119	12	1999.07.26.23	Neil, 9905
13	1992.08.18.19	Kent, 9211	13	2002.07.05.10	Rammasun, 0205
14	1992.09.24.02	Ted, 9219	14	2002.08.31.09	Rusa, 0215
15	1993.08.10.00	Robyn, 9307	15	2006.07.10.00	Ewiniar, 0603
16	1995.08.24.23	Janis, 9507	16	2006.08.19.10	Wukong, 0610
17	1999.08.02.08	Olga, 9907	17	2010.08.10.21	Dianmu, 1004
18	1999.09.19.15	Ann, 9917	18	2010.09.06.16	Malou, 1009
19	1999.09.23.19	Bart, 9918	19	2011.08.07.13	Muifa, 1109
20	2000.07.10.09	Kai-Tak, 0004	20	2012.07.18.18	Khanun, 1207
21	2000.09.15.11	Saomai, 0014	21	2014.08.02.07	Nakri, 1412
22	2003.06.19.00	Soudelor, 0306	22	2014.09.23.17	Fung-Wong, 1416
23	2003.09.12.14	Maemi, 0314	23	2015.07.12.03	Chan-Hom, 1509
24	2004.06.20.12	Dianmu, 0406	24	2017.07.03.19	Nanmadol, 1703
25	2004.07.04.05	Mindulle, 0407	25	2018.07.03.07	Prapiroon, 1807
26	2004.08.18.02	Megi, 0415	26	2019.07.19.21	Danas, 1905
27	2004.09.06.22	Songda, 0418	27	2019.08.11.14	Lekima, 1909
28	2005.09.06.05	Nabi, 0514	28	2020.08.05.00	Hagupit, 2004
29	2007.09.16.05	Nari, 0711			
30	2010.09.01.14	Kompasu, 1007			
31	2011.06.25.21	Meari, 1105			
32	2012.08.27.17	Bolaven, 1215			
33	2012.08.30.01	Tembin, 1214			
34	2012.09.16.22	Sanba, 1216			
35	2015.08.24.22	Goni, 1515			
36	2018.08.23.01	Soulic, 1819			
37	2019.08.15.04	Krosa, 1910			
38	2019.09.22.05	Tapah, 1917			
39	2020.09.02.16	Maysak, 2009			
40	2020.09.06.22	Haishen, 2010			